C.P. No. 1117

C.P. No. 1117

MINISTRY OF TECHNOLOGY

AERONAUTICAL RESEARCH COUNCIL

CURRENT PAPERS

An Investigation of the Stresses in a Wind Tunnel Corner Section

by

D. E. W. Stone and P. S. A. Baxter

Structures Dept., R.A.E., Farnborough

LONDON: HER MAJESTY'S STATIONERY OFFICE

1970

PRICE *15s 0d* [*75p*] NET

U.D.C. 533.6.071.1 : 533.6.048.6 : 531.218 : 531.259.223 : 539.319

C.P. No.1117*
February 1969

AN INVESTIGATION OF THE STRESSES IN A WIND TUNNEL CORNER SECTION

by

D. E. W. Stone
P. S. A. Baxter

SUMMARY

This Report describes how the stresses in a wind tunnel corner section were investigated by means of a 1/6 scale model. Both the brittle coating technique and elevated temperature strain gauges were employed. Two separate tests were performed in which it was attempted to simulate the thermal stresses and the pressure stresses respectively. Methods of overcoming some interesting experimental problems are fully reported and the significance of the results obtained is discussed.

---

* Replaces R.A.E. Technical Report 69021 - A.R.C. 31468

CONTENTS

1 INTRODUCTION

A new high speed wind tunnel has recently been installed at the National Physical Laboratory, and during commissioning some anxiety was expressed about the stress situation in one particular section of this tunnel, namely the corner section of the heat transfer tunnel. This corner section is subjected to quite high [800 lbf/in^2 (5510 kN/m^2)] working pressures as well as severe temperature gradients. It had successfully undergone a proof pressure test to 1020 lbf/in^2 (7030 kN/m^2), although it was noted that there was excessive bending in the flanges at this pressure and gussets were later attached to reduce this.

Strain gauge results were available[1] for an internal pressure test on a somewhat larger but basically similar corner section, which had been built for a cascade corner bend in a nuclear power station. These results revealed tensile stresses as high as 34000 lbf/in^2 (244000 kN/m^2) at a pressure of 700 lbf/in^2 (4830 kN/m^2) during its proof test. Above this pressure yielding took place and the gauge readings no longer increased linearly with pressure. It was considered that similar stress levels might exist in the N.P.L. corner section, and it was not known what effect the additional thermal stresses, arising from the temperature gradients, would have. In view of this it was decided to attempt to investigate the stress situation experimentally by means of a 1/6 scale model, and Structures Department, R.A.E. agreed to carry out the experimental programme.

2 DESCRIPTION OF THE PROTOTYPE AND MODEL

The corner section consists of a spherical shell pierced by two similar stub cylinders whose axes are at right angles. Fig.1 shows the model and it can be seen how there are reinforcing rings at the two intersections. Flanges are welded at the outer ends of both cylinders and these are drilled to take clamping bolts and recessed to receive a sealing ring. The flanges are not of equal outside diameter or thickness because, in the prototype, these flanges are used to connect the corner to two branch pipes containing the "mixing" and "settling" chambers respectively. The latter is heavier and is therefore connected to the larger flange.

In the 1/6 scale model it was not considered necessary to reproduce the branch pipes in detail and the "mixing" and "settling" chambers were simply represented by cylinders of differing diameters, the ends of these cylinders being sealed with end plates. (For dimensions see Figs.1 and 2.) This

arrangement can clearly be seen in Figs.3 and 4 which show the model during the thermal stress test. The end plates were drilled and tapped to take suitable fittings for pressurising the assembly, measuring the pressure, and sealing around the leads to the internal strain gauges. Air bleed cocks were provided in both flanges and an internal tube from one end plate to the top of the spherical section allowed any air trapped there to be removed.

The model was made of mild steel to BS1501 and great care was taken during fabrication to ensure freedom from residual fabrication stresses. The spherical shell was normalised after hot forming and then stress relieved after welding and prior to machining.

3 TEST PROGRAMME

The stresses produced in the corner section arise from three main sources (i) internal pressure (ii) temperature gradients and (iii) mechanical loading introduced through the cylindrical arms. As explained above, it is unlikely that there will be significant residual stresses, and observation of some strain gauge outputs while tightening the flange bolts indicated that the stress at the gauge points was hardly affected. Also observation of the prototype led to the conclusion that (iii) was of minor importance and it was decided only to attempt to reproduce (i) and (ii) on the model. It would, of course, have been possible to simulate both of these effects at the same time, but in order to obtain representative temperature gradients it would have been necessary to employ air instead of water for pressurisation. The necessary safety precautions associated with air pressurisation would, however, have considerably increased the difficulty of testing, and it was felt that the two effects could satisfactorily be tested separately and then superimposed.

3.1 Proof test

Although grooves for sealing rings were machined in the flanges of both branch pipes no suitable sealing rings were provided when the model was sent from N.P.L. It was decided therefore to see if simple gaskets cut from "Hallite" sheet material would suffice, and these were used when bolting the model together. Difficulty of access prevented a torque-spanner being used on the clamping bolts, but as far as possible it was ensured that all bolts were equally tight. The model was then filled with water and a manually operated single-acting boiler testing pump was connected to an end plate fitting. A similar fitting was connected to a robust pressure gauge and a low pressure applied to allow any trapped air to be bled off at the three points provided.

To ensure the safety of the model in later tests a simple proof pressure test was performed out of doors with the model surrounded by sandbags and the pump operated from a remote protected position. Although the gaskets leaked a little this did not prevent the proof pressure of 1020 lbf/in^2 (7030 kN/m^2) being applied without failure. Care was taken not to exceed 80% of this value in any subsequent tests.

3.2 Initial brittle coating test and selection of strain gauge positions

The results already obtained on the nuclear power station cascade corner section[1] gave a good indication of areas of likely importance, but before selecting positions for the attachment of strain gauges on the model it was felt desirable to perform a pressure test with a strain sensitive brittle coating on the model. The surface condition of the model was not as good as might have been desired and it was cadmium plated and polished before coating to remove minor irregularities and to provide a reflective surface. The coating employed was the R.A.E. water based brittle coating[2] and the usual application procedure was adopted.

The results obtained can best be described with reference to Fig.2. It should be noted that the centre-lines of both branch pipes lie in a horizontal plane and that the vertical centre-line of the corner is taken as the vertical line passing through the point of intersection of the centre-lines of the branch pipes. (The latter point does not quite coincide with the centre of the sphere.) The strain gauge results in Ref.1 indicated that the maximum tensile stress occurred at a point (2); i.e. at a point on a vertical plane through Y-Y lying on the upper surface of the sphere near to its junction with the reinforcing ring. This stress was in the direction YY, but an equal tensile stress was found in the perpendicular direction. The stress on the inside surface was shown to be similar but slightly less, and in view of this it was decided only to fix a pair of external strain gauges at this point on the model.

The brittle coating test on the model, however, indicated that the maximum tensile strain occurred in a vertical direction at point (6); i.e. at a point in the horizontal plane containing the branch-pipe centre-lines and lying on a radius of the sphere inclined at 45° to both these centre-lines. It was decided therefore to fit a pair of gauges at this point, having horizontal and vertical orientations respectively; a similar pair was attached internally. To monitor the membrane stress in the sphere a pair of external gauges was also attached at point (1), which was in the same horizontal plane

but lay on a radius making 135° to the centre-lines. The brittle coating results also showed that there were high tensile circumferential strains near the flange on the stub cylinder leading to the larger branch pipe. Pairs of external gauges were fixed in both the circumferential and longitudinal (Y-Y) directions at points on the surface of this stub cylinder lying in the plane X-X. The positions of these points (3), (4) and (5) are shown in Fig.2. Similar internal gauges were fixed at points (3) and (5) only. Gauge positions and orientations will be specified as 5BE, 5TI etc., the number indicating the point on the model, B or T the orientation (see Appendix A), and E or I showing whether the gauge was external or internal.

The short gauge-length, elevated temperature, strain gauges were not very robust and attaching the leads required great care. This was especially true in the case of the internal gauges because of the confined space and restricted vision. The technique of attaching the gauges is also described in Appendix A. In two cases (2BE and 6TE) one of a pair of gauges at a particular point failed before the tests but, because of the difficulty of replacement, it was decided to continue without them.

3.3 Thermal stress test

In order to provide correct simulation of the temperature gradients in the model it was necessary to take temperature measurements on the prototype. The wind tunnel had not been run at maximum temperature and pressure, but a fairly detailed temperature distribution had been obtained during tests of the electrical preheating units with the control units set for the maximum working temperature of 450°C. Also measurements made at pressures up to 120 lbf/in^2 (827 kN/m^2) and 350°C had suggested that the temperature distribution within the structure was broadly similar to that observed during the preheater trials. It was felt, therefore, that it would be reasonable to attempt to reproduce this distribution on the model.

It was obviously not necessary to reproduce the absolute temperatures since the magnitudes of thermal stresses are governed only by the temperature differences from point to point, (apart from the effect of the absolute temperature on the elastic constants and on the yield stress). The temperature measurements made on the prototype enabled the temperature differences between eight different points on the model to be specified, see Table 1. The maximum temperature difference was, however, 170°C and preliminary trials showed that it would not be easy to reproduce this in the laboratory. The initial limitation was the fact that the strain gauge cement combination selected (see

Appendix A) was only usable up to 180°C. It was hoped to overcome this simply by cooling localised areas below ambient temperature so as to obtain the required temperature difference without exceeding the prescribed maximum, but it eventually proved impossible to attain the maximum temperature with the available radiant heaters. This problem could, no doubt, have been overcome by the use of more elaborate forms of heating, but it was felt that quite satisfactory results could be achieved if all the temperature differences reproduced on the model were made exactly one half of those on the prototype. The factored values of the prototype temperature differences together with those measured experimentally using thermocouples welded on the model are given in Table 1. These values were attained quite readily by means of a number of radiant heating lamps together with cooling by ducted room-temperature air at point (6). This arrangement may be seen in Figs.3 and 4, although some thermal insulation has been removed from the region of point (6) to allow the cooling arrangement to be seen more clearly.

The test procedure ensured that the gauges and dummies had been connected in circuit for at least an hour before the individual apex resistors were adjusted to zero each gauge; by this means it was hoped that stable initial temperature conditions had been achieved. The heating lamps and blower motor for the cooling air were then switched on, and the thermocouple readings checked from time to time until stable conditions were obtained. This usually required 2-2½ hours and it was then necessary to make minor adjustments to the lamp positions in order to get the exact temperature distribution required. Time was then allowed for the situation to restabilize before recording the temperatures and taking all the strain gauge readings. The lamps were then turned off but the cooling air was still supplied for a further half hour. This too was then turned off and the model allowed to cool naturally to room-temperature, when the strain gauges were read once more.

In fact, however, it was difficult to perform the whole of this test in one day, largely because of the time taken to cool to room temperature after the tests. If the final zero readings were taken on the following morning, after allowing the usual time for the gauges to warm up, it was found that considerable drift had taken place overnight. It was felt that the gauge-cement combination employed might not have been satisfactory and that creep of the cement might have taken place; other possible sources of drift lay in the strain gauge bridge itself. With this in mind a fairly detailed investigation of these problems was initiated, and this is described and discussed in

Appendix B. A number of test runs of the type described were also made and it was eventually concluded that reasonably reliable results were obtained from readings taken before and after the heating phase. Measurements for the cooling phase also appeared quite satisfactory if the final zero readings were taken on the same day as the rest of the test. At the end of the day the temperature of the whole laboratory had increased, and the sphere was usually about 5°C above its initial temperature; there was, however, usually less than 3°C temperature difference between any of the thermocouples or the sphere itself, although there might still be as much as 10°C difference on the branch pipes. Under these circumstances the average zero error was about -25 $\mu\varepsilon$ (which is largely accounted for by the increased temperature), with a maximum error of -50 $\mu\varepsilon$.

The results of the run considered most reliable are listed in Table 2. The measured strains were first corrected by taking into account the apparent strain caused by the increase in temperature (available as a calibration curve with each batch of gauges), and then doubled to allow for the fact that only half the true temperature difference was produced on the model. It is this final value which is listed in the table and which was used to calculate the stresses.

3.3.1 Discussion of thermal stress test results

Before considering the results it should be noted that the gauges were fixed in pairs at each point, the directions of the gauges being aligned along the principal axes of strain as indicated by the brittle coating. It is possible that in some cases the principal axes of the thermal strains did not coincide with the gauge axes, although on the spherical portion the major thermal strain was created by the temperature differences between points on the sphere lying on a vertical plane Z-Z through points (1) and (6). Thus symmetry about this plane might be expected.

In general the measured thermal strains were quite low. In fact, in many cases, the corrections for the apparent strains induced by the elevated temperature were of the same order as, or even greater than, the measured strains. Not surprisingly, a non-uniform biaxial stress state was produced at point (1), the greater stress lying on plane ZZ. At point (6) however, the diametrally opposed point in this plane, the higher compressive stress was produced in a direction perpendicular to the plane. This would not of course seem unreasonable in view of the high degree of local constraint in this region, but it is unfortunate that the external gauges at this point failed before satisfactory readings were

taken, because they would have enabled the degree of local bending to be determined. The other gauge point on the spherical portion of the model is point (2). Here again stresses are only obtainable for the inside surface and it can be seen that moderate tensile stresses are produced. The directions of the principal axes at this point are uncertain and the value of the major principal stress could well have been somewhat higher than the value recorded in Table 2.

It is interesting to compare the stress situations at the two diametrally opposed points (3) and (5). At point (3) which is remote from the complex constraints at point (6) there is a mean tensile circumferential stress of about 2300 lbf/in^2 (16000 kN/m^2) with very little local bending to give a variation through the thickness. The mean longitudinal stress is low, being only -600 lbf/in^2 (-4100 kN/m^2), and there is also little local bending in that plane. At point (5), however, the mean circumferential stress has dropped to 1600 lbf/in^2 (11000 kN/m^2), but there is a strong degree of local bending, ±3300 lbf/in^2 (23000 kN/m^2). Similarly the mean longitudinal stress has increased to 3400 lbf/in^2 (24500 kN/m^2), the local bending being 2400 lbf/in^2 (16500 kN/m^2). It is difficult to postulate how the applied temperature distribution created this situation, and it can only be stated that, although the stress pattern is complicated, there do not appear to be any large tensile stresses.

3.4 Internal pressure test

As is explained in Appendix A the PTFE covered wire used for the elevated temperature testing was found unsuitable for the subsequent internal pressure test because it allowed water to enter and eventually led to the necessity for replacing all of the internal gauges. A preliminary pressure test was made, however, with readings taken only on the external gauges (apart from some rough readings on 6BI and 6TI before these two failed). For this test an accurately calibrated pressure gauge having a maximum capacity of 750 lbf/in^2 (5170 kN/m^2) was substituted for the more robust gauge used on earlier tests and this was used on all subsequent tests. More complete tests are described below and the results of this preliminary test will not be tabulated, but reference will be made to them later.

As was mentioned in section 3.2, considerable difficulty was encountered in cementing and wiring the internal gauges and an encapsulation technique was developed to ameliorate this when attaching fresh gauges. This technique, together with the methods used for waterproofing, are described in Appendix A.

Despite this a little water managed to penetrate between the wires and the PVC insulation for some gauge leads, but the gauges continued to operate satisfactorily. Also because of the necessity to maintain the pressure for some minutes while the strain gauge readings were being taken, the gaskets were replaced by rectangular section rubber sealing rings cut to fit the 0.10 inch (2.5 mm) deep grooves in the branch-pipe flanges. Two different thicknesses of material were available for these sealing rings and at the time it did not appear to be important which of these was used. Because of this, thin (0.13 inch, 3.3 mm) seals were used throughout except on the flanged joint between the settling chamber (large) branch pipe and the spherical corner, for which a thick (0.20 inch, 5.1 mm) seal was used. All the flanged joints sealed quite satisfactorily and metal-to-metal contact was made at all of them, except that containing the thick sealing ring which allowed a small degree of flexibility.

Before beginning the test the internal pressure was cycled several times to the maximum value. An internal pressure test (Test 1) was then performed, taking strain gauge readings at a number of pressure increments up to a maximum of 750 lbf/in^2 (5170 kN/m^2) and these are plotted in Figs.5 to 13. Similar readings were also taken for decreasing pressure; these are not plotted but it may be stated that they were generally similar to the values for increasing pressure, although a degree of hysteresis was noted in some cases. On comparing the external gauge readings taken on this test with those taken on the preliminary test mentioned earlier in this section it was found that some discrepancies existed. Without exception the results obtained on the later test were more linear than those from the preliminary test, but in some cases the magnitudes of the measured strains differed considerably. In particular the values for 3BE, 4BE and 5BE increased by 60-65%. Also 4TE and 6TE, which were small on the preliminary test, became very small indeed. The results from the other gauges remained sensibly unchanged. On examination of the results obtained on the internal gauges it was at once apparent that 3TI and 5TI were exhibiting gross initial non-linearity; slight non-linearity was also exhibited by 3TE and 5TE. A repeat test, however, confirmed all of these results.

It was suspected that the strange results on 3TI and 5TI might be attributed to malfunctioning of the strain gauges, but the fact that these initial non-linearities were of opposite sign for two diametrally opposed points did indicate that the gauges could truly be recording some initial warping of the joint. To investigate this further the thick seal was replaced by a thin one and the flanges tightly bolted together, giving clamping conditions more

closely approaching those obtained in the preliminary test. An identical internal pressure test (Test 2) was then performed and the readings obtained are compared with those from Test 1 in Figs.5 to 13. The results of both Test 1 and Test 2 are listed in Table 3 which also shows the calculated stresses, wherever both gauges in a pair were operational.

3.4.1 Discussion of pressure test results

In Test 2 the results for the external gauges were found to be very similar to those obtained on the preliminary test, although they were a good deal more linear. This is again demonstrated most clearly by comparing the results for 3BE, 4BE and 5BE in Tests 1 and 2 (see Figs.7, 9 and 10). It may be seen how the strains recorded for these gauges in Test 1 were 60-65% higher than those for Test 2. Examination of the corresponding longitudinal gauges shows that both 3TE and 4TE, although not of very great magnitude, exhibited an even greater increase and in fact changed sign; 5TE, however, remained virtually unchanged. The remaining gauges showed little difference in the two tests with the exception of 6TE, which gave only small non-linear readings in both tests, a higher value being shown in Test 2.

Before considering the above results in terms of stresses the strains recorded from the internal gauges will be considered. At point (2) 2BI failed before the test; 2TI, however, gave a good linear relationship in Test 1, but the output in Test 2 was low and non-linear. Gauge 3BI failed during the pre-cycling before Test 1, but some readings were taken during these tests and since these proved to be fairly linear it was decided to include them in Table 3. Although these results were obtained with the thin sealing ring, and thus are really only valid for Test 1, they have also been inserted in the table for Test 2 so as to enable the stresses to be estimated. It will be seen later, however, that the validity of such estimates is very doubtful. Comparison of the results of both tests at 5BI suggests that this substitution might not be unreasonable. Strange results were obtained on 3TI and 5TI (see Figs.8 and 11); gross initial non-linearity was observed in both tests and for each gauge this proved to be repeatable in each test and of the same form in both tests. Some time later, when the model was finally stripped it was noticed that the adhesion at the internal gauges had deteriorated. The encapsulation had remained intact and there was no sign of any water penetration between it and the Araldite strain gauge cement which was used to attach it to the model. The interface between the strain gauge cement and the steel surface of the model, however, showed clear signs of penetration and the encapsulations

at points (3) and (5) were able to be peeled from the surface without the application of undue force. It seems likely therefore that the observed non-linearity can be attributed to a partial failure of adhesion. The repeatability of the results does indicate that the situation was stable at the time of the tests and it may be suggested that the final (linear) portion of the curves are probably indicating the true behaviour. In view of this, the results for the internal gauges at points (3) and (5) have been presented in two ways in Table 3. The results using the actual readings are included in the usual way but another figure is entered in brackets below them. This figure is the reading which would have been obtained if the gauge output had been linear throughout (taking the slope of the final, linear, portion).

The stresses calculated from the strain gauge readings have been made nondimensional by expressing them as σ/p where σ is the stress in a given direction and p is the applied internal pressure of 750 lbf/in^2 (5170 kN/m^2). As would be expected the membrane stress at point (1) is an equal biaxial stress $\sigma_m/p = 13.9$, which compares quite well with the predicted value from simple shell theory of $pd/4t = 14.2$.

For the stub cylinder, however, the situation was considerably more complex. Only external gauges were attached at point (4) and these will not be considered except to point out that the readings obtained are fully consistent with those from the external gauges at point (5). The complex constraints at point (5), however, introduce a high degree of local bending and it was felt that the interpretation of these results might be assisted by an approximate theoretical assessment of the stress pattern. The geometry of the stub cylinder makes this difficult, since one end is perpendicular to the cylinder axis whilst the other is inclined. Appendix C, however, gives an analysis for thin cylinders of different lengths with various degress of end restraint the results of which are shown in Figs.14 and 15.

This analysis can of course only be of general guidance, since it considers a uniform thin cylinder with both end faces perpendicular to the cylinder axis, but the maximum and minimum lengths selected for use in the calculations are approximately the lengths, at position (3) and (5) respectively, of the stub cylinder. Thus in the analysis both $\sigma_{\ell b}$ and σ_c only vary with distance along the length of the cylinder and not with location around the circumference. (Suffices ℓ and c refer to the longitudinal and circumferential directions respectively and b signifies bending.) It must also be pointed out here that at all gauge locations the top and bottom gauges were

alongside one another and not superimposed; thus they measured the strains at slightly different points. This is not important for some locations, but at points (3) and (5) the theoretical analysis indicates that the strain pattern varies quite rapidly from point to point and it is not possible to calculate the stresses at these positions from the strain gauge readings. Ignoring the presence of the weld fillet, the approximate lengths of the stub cylinder at positions (3) and (5) were 1.60 and 1.00 respectively. If, as in the analysis, x (longitudinal) distances are measured from the mid-length position, and if distances towards the branch pipe are taken as positive, then the positions of the strain gauges were 3B x = 0.21, 3T x = -0.10, 5B x = 0.06, 5T x = -0.38.

The theoretically determined stresses may be used to predict the strain distributions which would be produced by a given set of boundary conditions. Such predictions are listed in Table 4 and it must be noted that the circumferential strains at each point have been calculated at the position of the bottom gauge and the longitudinal strains have been calculated at that of the top gauge. Where any question of non-linearity exists for the measured values (i.e. 3TI and 5TI) the assumed linear value, which is the figure in brackets in Table 3, has been taken.

The uncertainty about the accuracy of the measured values for 3BI and 3TI suggest that it would be more valuable to examine the comparison of predicted and measured values for gauge position (5). The most obvious difference between these values lies in the fact that the measured values exhibit a marked degree of circumferential bending. Appendix C shows that bending moments M_x and M_ϕ exist, thus proving that there are bending stresses in both the longitudinal and circumferential directions. Table 4 shows, however, that when these two bending stresses are combined with their corresponding direct stresses the resultant circumferential strain has no bending component. Such a result would of course be expected from the given conditions of axial symmetry. In the case of the model, however, the cylinder length varies with ϕ. Thus for a given value of x, M_x (and hence $M_\phi = \nu M_x$) will also vary with ϕ. This variation is not dealt with by the simple analysis, but it can be seen how circumferential bending strains can be developed.

The mean measured circumferential strain of 323 $\mu\varepsilon$ for Test 1 is, however, quite near that of 360 for the boundary condition (1) (completely free). The greater end restraint introduced by this seal in Test 2 reduced this mean value to 163 $\mu\varepsilon$ and also reduced the superimposed circumferential bending from $\pm$662

to ±497 με. It is interesting to note that the theoretical results show that the introduction of some end restraint (condition (2)) reduces the circumferential strain to 75 ∓110 με and that further restraint (condition (3)) reduces it still further to -25 ∓45 με. Thus both the mean value and the superimposed bending are decreased by increasing the end restraint, although in this case the bending is of the opposite sign.

The longitudinal strains are rather more difficult to reconcile because the measured results for both tests give a mean strain of almost zero with a superimposed bending of about ±240 με. This bending strain is of the same order and sign as that predicted for condition (2). Virtually no direct tensile strain was measured, however, and it is difficult to conceive conditions which could create this situation.

The results obtained at position (6) during Test 1 are quite reasonable; the uniform biaxial stress system exhibited at position (1) has been increased by the local constraints and local bending has taken place in the direction of the top gauges (i.e. in the plane of the branch pipes). Unfortunately Test 2 indicated that, whilst the readings of the external gauges remained substantially unchanged, those of the internal gauges changed sign. This indicates that stiffening one of the flanged joints can drastically modify the stress distribution in this area. Since this conclusion entirely rests on the results obtained from the internal gauges at this position, it may be suggested that further verification is desirable before such a conclusion could be accepted. It may be of interest to note that a 1 inch gauge length Huggenberger gauge, placed so that it both straddled gauge No.18 (6BE) and was aligned with it, recorded a strain of 480 με. This approximately confirms the strain gauge reading and indicates that there were probably no high strain gradients in this direction.

3.4.2 A comparison of brittle coating and strain gauge results

Since the brittle coating test gave an overall picture of the strain distribution on the outside surface of the model and enabled the regions of largest tensile principal strain to be identified, it is interesting to examine how closely these results correlate with the corresponding strain gauge readings. Such a comparison is made in Table 7 but, because of the probable effect of the clamping conditions at the flanged joints, the strain gauge readings presented are those obtained on the preliminary pressure test, which was performed under exactly the same conditions as the brittle coating test. In fact, comparison with Table 3 shows that the results for the preliminary test and for Test 2 were very similar.

If it is remembered that the threshold strain of the brittle coating cannot be specified to an accuracy of better than ±50 με then quite acceptable agreement is seen to have been obtained for most positions. Only for position (6) was there a large discrepancy. At this position the coating cracked at a low applied pressure, thus indicating a high surface strain. It may be noted, however, that some difficulty was experienced in spraying an even coating onto this particular area because of the difficulty of access. Also the reinforcing rings tended to mask this region. It is therefore possible that the coating was not sufficiently thick in this region, and this would have the effect of making the coating locally too sensitive. The results obtained with a Huggenberger gauge, reported in the previous section, tend to support this conclusion.

4 CONCLUSIONS

This investigation, which was apparently straightforward, introduced a considerable number of unexpected experimental difficulties, the majority of which have been overcome. It has been shown that the general level of thermal stress is low and that the maximum measured thermal stress (at position (6)) was compressive. It would, however, be valuable to determine the degree of thermally induced local bending in this region.

The results of the internal pressure tests did not reveal any unduly high stresses at position (6), but it must be borne in mind that these will be superimposed on the thermal stresses which are to some extent still undetermined. The stress distribution in one of the stub cylinders has been considered in some detail and it is shown that quite high stresses can exist. An approximate theoretical analysis has demonstrated how high stress gradients can be produced, but it must be stated that there was little evidence of this in the crack patterns obtained in the brittle coating test. In the prototype local stress raisers such as welds could also modify these stresses. The importance of the flange stiffness on the stress distribution has also been shown and it should be noted that in this respect the model is somewhat different from the prototype, in which the flanges were stiffened by gussets (see section 1).

It was hoped to do a further brittle coating test in which special attention would have been paid to the region of the stub cylinder, but non-availability of plant has made this impossible. It can therefore only be suggested that a limited number of results from strain gauges attached to the prototype, at positions selected in the light of this Report, would be extremely valuable. It is not the function of this Report to discuss failure

criteria but it seems likely that under the elevated temperature operating conditions some local yielding will take place which could modify the stress distribution. Such yielding might well be beneficial in eliminating local stress concentrations near welds, but its effect on the bending of the stub cylinders produced by the flange constraints is less certain.

Appendix A

THE STRAIN GAUGE INSTALLATION

A.1 Introduction

It was hoped to select and install a strain gauge system which would be usable at elevated temperatures for the thermal stress test, and yet which would also be able to be waterproofed satisfactorily for the later internal pressure test. A wide range of strain gauges is, of course, commercially available, and it would have been possible to obtain suitable temperature compensated gauges from a number of different manufacturers. It was decided, however, to use gauges manufactured by Automation Industries (U.K.)*, because gauges of this type had recently been used satisfactorily on other projects and they were available from stock. The particular gauge type selected was C6 124-A, which is temperature compensated for use on steel and consists of a Constantan foil element on an epoxy-fibreglass backing, making it suitable for use up to 180°C. The gauge length is $\frac{1}{8}$ inch, the gauge resistance 120 ohms and the gauge factor 2.06. The suffix A indicates that the grid is narrower than standard.

The recommended cement for use with these gauges is Budd GA-60 epoxy cement. This requires the application of pressure while the cement is cured for three hours at 180°C, (for service up to 150°C), and it was eventually decided, in the light of past experience, that it would be preferable to use Shell Epikote 828, plus hardener M (44 p.b.w. hardener to 100 p.b.w. resin)** Less pressure was required with this cement and it was found satisfactory to hold the gauges in position by placing a suitably contoured pad of silicone rubber on top of the gauge and taping this to the model surface with high temperature silicone tape. The cement was cured in two stages. The model was first soaked for 4 hours at 60°C and then the temperature was slowly increased to 180°C and the model soaked for a further 2 hours.

In all cases the gauges were attached in pairs, the gauge backing being trimmed by hand to align the two grids and to bring them closer together as shown in Fig.16a, so that the projection of the axis of the "top" gauge always bisected the gauge length of the "bottom" gauge. The orientation of the "top" and "bottom" gauges at each point on the model is given in Table 2. Only at point (6) was there insufficient room for this layout, and here the gauges were arranged as shown in Fig.16b.

---

* Formly Budd Instruments (U.K.).

** p.b.w. = parts by weight.

Because the model would be subjected to elevated temperatures PTFE insulated wire was used to connect the gauges to a plug panel; multicore PVC covered cables led from this plug panel to the measuring bridge. The lack of accessibility made it extremely difficult to solder the leads on to the internal gauges but, with the aid of a mirror and a suitably cranked soldering iron, this was eventually completed. All the gauges were then waterproofed with Budd Waterproofing GW-4. The external leads were secured by specially prepared clamps which had been cemented to the surface of the model, but internally this was not readily possible and the leads were secured instead by small quantities of Dow Corning RTV 731 silicone rubber. To protect the internal gauges and soldered joints they were also covered with RTV 731.

A.2 Thermal stress test

It was obvious that the temperature, and hence the resistance, of the gauge lead wires would change during the thermal stress test, and it was therefore necessary to use a three wire system for connecting the gauges into the bridge. (See Fig.18.) This ensured that one lead of each active gauge lay in the dummy arm of the bridge. For the external gauges this only meant attaching an extra lead to one of the gauge terminals, but the difficulty of access to the internal gauges made this impracticable. For the latter a compensating loop of identical lead wire was laid alongside each pair of leads and this was connected into the appropriate dummy circuit. By these means, full temperature compensation was obtained for all the leads. Ordinary wire wound resistors were used as dummy gauges. These were mounted on a suitable insulated block and sealed in a test tube with a little silica gel to remove any moisture. The test tube was then suspended in melting ice in a vacuum flask and by this means it was felt that the dummy resistances remained sufficiently constant.

The remainder of the bridge was made up by a Doran bridge unit, which contained the calibrated slide wire and two standard 200 ohm arms. With a 3 wire system it is not possible to use the usual set of apex units and the bridge could only be zeroed by shunting one of the standard arms with a resistance box. This proved to be quite repeatable, but it was wondered whether this shunt resistance would vary significantly with room temperature. Tests showed, however, that a change in room temperature of 10°C would only produce a change in resistance of the standard arm of 12 $\mu\Omega/\Omega$. Thus errors from this source would be negligible. The bridge was fed with 1.0 V from a stabilized power pack, and a switch was fitted which allowed the polarity to be reversed. For the thermal stress tests readings for each gauge were taken

with both positive and negative supply polarity and the mean value was taken. This ensured that the effects of any thermal emf in the bridge circuit or the galvanometer circuit were eliminated.

It can be seen from Figs.3 and 4 that it was necessary to place the radiant heating lamps quite close to the model in order to achieve the required temperature distribution, and, in order to minimise the effect of direct radiation on to the external gauges, each gauge was covered with a small rectangle of reflective backed self-adhesive tape. Similar precautions were also taken with the thermocouples.

A.3 Internal pressure test

Since the pressure test would be at constant temperature it was not necessary to use a 3 wire system and all the third wires and compensating loops described in A.2 were removed. All exposed junctions at the internal gauges were coated with the Dow Corning silicone rubber. The remaining leads to the internal gauges had been specially arranged in two looms of eight leads each, and before connection to the gauges each loom had been fitted with a specially designed pressure seal to allow the leads to pass through the end plate. The construction of the end plate fitting is shown in Fig.17. To form this seal a 2 inch (5 cm) length of each PTFE covered wire was etched with a solution of sodium, tetrahydrofluorine and napthalene. Each batch of eight leads was then passed through a conical mould and assembled in a special jig which held them at a suitable angle and spacing. The mould was then filled with silicone rubber (Midland Silicones Cold Cure Silastomer 9161) which was allowed to cure for 12 hours at room temperature. The assembly jig ensured that each lead was entirely surrounded by the silicone rubber and avoided the creation of voids A thin nylon washer was jig-drilled to accept the wires and, when the nut on the end plate fitting was tightened, this washer pushed the conical seal firmly into its seating. The conical shape of the seal ensured that it became more effective as the pressure increased. It was, of course, necessary to fit this seal to the end plate before the latter was bolted on to the branch-pipe.

The strain gauges were then given a more thorough waterproofing treatment by covering them with a liberal coating of "Rito" bitumastic compound. To prevent the "Rito" being washed away when the water was pumped in, it was covered with a square of bandage which was taped down at its edges. This system had previously been used satisfactorily up to pressures of 700 lbf/in^2 (4830 kN/m^2) and was thought to be quite suitable for these tests. The model was then assembled and filled with water. At this stage the resistance of the

gauges and their insulation resistance to earth were checked and found to be satisfactory. As soon as pressure was applied, however, water was seen to be coming from the outer ends of the PTFE wires, and before long all the internal gauges had shorted to earth.

The model was stripped down and the gauges carefully examined. It was found that, although water had penetrated inside the PTFE insulation of the lead wires, it did not appear between the top surface of the gauge and the waterproofing layer. When the "Rito" was removed it was found that the silicone rubber had lifted and that some of the internal gauges could be removed without much difficulty. It is suggested that this can be explained by some form of migration taking place from the silicone rubber, producing adverse effects at the metal/cement interface. This phenomenon has since been observed to take place on other elevated temperature installations using Philips 'E' (a three component polyester adhesive). The failure of the internal gauges, however, was not from this cause but from the penetration of water into the leads. The PTFE coating on these leads is quite thin and it was felt that the etching process might have produced pin-holes through which the water could have entered. Simple immersion tests confirmed this, and it was therefore decided to replace the wiring looms with new looms assembled from leads having a thicker PVC insulation. This PVC insulation was considerably more robust and did not require etching to achieve satisfactory adhesion to the conical silicone rubber seal. (It could not, of course, have been used for the thermal stress tests, because it is not usable at the required temperature.)

It was then necessary to renew the internal gauges and, in view of the difficulties encountered during the first installation, it was decided to connect the leads to each pair of gauges and to encapsulate them in the laboratory before cementing the whole assembly into the model. Since the thermal stress test had been completed the new gauges did not have to satisfy an elevated temperature requirement, and the replacement gauges selected were type C6 121 which has a pure epoxy backing.

A.4 Encapsulation technique

Encapsulation procedures had previously been used for other applications but in all cases the surfaces had been flat or convex and a gauge, when held down at its ends, naturally followed the contour of the surface. For the present model, however the surfaces were all concave and in some cases possessed double curvature. It was therefore necessary to develop a new technique and the method finally used is described below.

Plaster moulds were cast which gave a replica of the concave surfaces at the gauge stations and the surfaces of these moulds were coated with "Certofix" (a water soluble glue). For each station a flat section of silicone rubber (ICI Silcoset 101) was cast in an appropriately machined perspex mould, giving the outline of the required encapsulation. This may be seen in Fig.19, and it should be noted how one area of this silicone rubber component is tapered. A pair of strain gauges were then lightly coated with "Certofix" and accurately positioned on the plaster mould. The silicone rubber component was then attached, formed to the concave contour and held in place by two clamps with screws passing through the plaster to a base plate. The gauge leads were also held by one of these clamps and were arranged so that the tinned ends of the leads pressed down lightly on the gauge terminals. If this precaution was not taken then there was a tendency for the leads to lift the foil of the gauge from its backing once the soldered joint had been made. The tapered section of the silicone rubber component ensured that the lead wires were directed away from the surface, thus allowing them to be entirely surrounded by the encapsulating resin when the mould was filled. A cover plate was also made to the correct curvature and its bottom face was sprayed with a PTFE release agent.

The resin used for encapsulation was a cold curing mix consisting of 9 p.b.w. hardener (HY 951) to 100 p.b.w. resin mixture (25% MY 750, 75% MY 753). (All these materials are manufactured by CIBA (A.R.L.) Limited.) The mix was thoroughly degassed before pouring, then the mould was carefully filled and the cover plate lightly clamped in position. 24 hours was allowed for the mixture to cure and then the cover plate, all the clamps and the base plate were removed. The remainder of the mould was placed in a shallow tray containing warm water of a depth not quite sufficient to reach the encapsulation. The water percolated through the plaster and dissolved the "Certofix" and after 15-20 minutes the encapsulated gauge was found to be readily removable. It was then thoroughly washed and dried.

It was felt advisable to give the resin a further cure at a slightly elevated temperature and so, because the encapsulation tended to soften and deform, it was temporarily replaced on an identical mould and lightly clamped in place using only the contoured cover plate. It was then given a post cure heat treatment of about 3 hours at 60°C, and when it was cool it was removed from the mould. The area of the mating face was very lightly abraded by hand using grade 400 waterproof paper. The encapsulated assemblies were finally cemented inside the model one at a time using dead weight loading to apply the

required pressure. No further elevated temperature testing was intended and so the cement used was Araldite strain gauge cement, which is an epoxy resin containing a filler. It was felt that this filler would help to minimise any inequality of curvature between the encapsulation and the model.

Appendix B

INVESTIGATION OF DRIFT PHENOMENA AND CEMENT CHARACTERISTICS

B.1 Drift phenomena

Section 3.3 describes how considerable drift in the bridge output was found to have taken place overnight. It was thought that this might be due to the measuring system and to investigate this a pair of temperature compensated 200 Ω gauges, which were available on a calibration bar, were wired into the circuit as an extra pair of active and dummy gauges. A standard thermal stress test was then performed and, as usual, by the end of the day the gauge readings had almost returned to zero. The output from the extra pair of gauges was checked and found still to be zero. Two days later the readings were rechecked and, whilst the extra gauges still read zero, the remaining readings were found to have changed radically. This indicated that the source of the drift lay in either the active gauges themselves or in the dummies.

A pair of 120 Ω gauges (C6 121) on a calibration bar was then prepared and one of these was used to replace an active gauge, retaining the usual dummy; the other gauge on the calibration bar was used to replace a dummy gauge for another position, retaining the usual active gauge. A further thermal stress test, however, demonstrated much the same behaviour on all gauges, irrespective of whether or not the gauges from the calibration bar were in the circuit. Because of this rather confused situation it was decided to investigate the behaviour of the selected gauge/cement combination.

B.2 Cement characteristics

To study the behaviour of the Shell 828 cement it was decided to compare its behaviour under the test conditions with a more recently available cement BR 600. This is a single component epoxy cement marketed by Welwyn Electric Limited. Two calibration bars were prepared each having two gauges cemented to it in such a way that they lay on the longitudinal centre-line and were symmetrical about the mid-length. First gauge (1) was attached to bar A and gauge (3) to bar B, using 828 cement and giving them the curing cycle specified in section B.1. Then gauge (2) was attached to bar A and gauge (4) to bar B, using BR 600 and curing for 1 hour at 110°C.

These calibration bars could be loaded in a simple cantilever bending rig fitted inside an oven. Two tests were carried out. In the first test, Test A, the gauges on bar A were used as active gauges while those on bar B served as dummies. It should be noted that the bending rig only applied a

given end deflection to the cantilever and it is possible that the clamping of the calibration bars could be slightly affected by a change in temperature. There was, however, little evidence of this. Gauge (2) behaved entirely satisfactorily throughout. The recorded resistance changes were of equal magnitude for loading and for unloading, and the values recorded with changing temperature were of the order given on the calibration sheet supplied with the gauges. Also there was little creep under load.

Gauge (1), however, which was fixed with the 828 cement exhibited a massive change in ΔR when the temperature was first increased to 89°C. This meant that all the remaining readings had to be taken on the less sensitive ranges of the measuring bridge but, even making allowance for this, the results were not at all consistent. In particular a high degree of creep was recorded. It was indicated therefore that the 828 cement was probably unsatisfactory for use at elevated temperatures, but it was decided to test bar B before coming to a firm conclusion.

The results of the test on bar B are given in Table 6 which gives the actual bridge reading $\delta R/R$ together with $\Delta(\delta R/R)$, the change in bridge reading between a given pair of consecutive readings. It may be seen that both gauges behaved perfectly satisfactorily, the changed recorded for increasing the decreasing load being virtually the same. The thermal outputs, the values of $\Delta(\delta R/R)$ produced by the change in temperature in the unloaded condition) from 24°C to 130°C, were small, and in the case of gauge (3) (cemented with 828) were very near the value of -150 $\mu\Omega/\Omega$ given in the calibration sheet supplied with the gauges. A measurable degree of creep was recorded under continuous loading at 135°C. The magnitude of this creep was, however, rather less for gauge (3) and very little further creep was observed after $1\frac{1}{2}$ hours under load. It must also be remembered that the strain produced by the applied load in this test was considerably higher than any of the strains measured in the thermal stress test (see Table 2), and any creep effects in the latter would be proportionately less. A similar test, the results of which are not tabulated in this Report, was also performed at 82°C and it was found that for this temperature the thermal outputs were only -75 and -40 $\mu\Omega/\Omega$ for gauges (3) and (4) respectively. Similarly a load was applied to produce 1000 $\mu\Omega/\Omega$ at gauge (3) and this value decreased by -40 $\mu\Omega/\Omega$ during the first $1\frac{1}{2}$ hours and thereafter remained constant.

The satisfactory test on bar B made the peculiar behaviour of gauge (1) on bar A seen questionable and Test A was repeated. It is the results of this repeat test which are given in Table 5. This time both gauges behaved satisfactorily although the thermal output from gauge (1) was rather higher than was expected. The degree of creep exhibited under a load sufficient to produce an initial value of 780 $\mu\Omega/\Omega$ at gauge (1) was negligible at 130°C. If gauge (1) had not been given a curing treatment at 180°C it would have been possible to suggest that the poor results in the original Test A were due to incomplete curing of the cement. Since this is not so, it can only be suggested that there could have been a fault in the gauge circuit. If so it was unfortunate that it should appear only when the temperature was raised.

It seems reasonable to conclude that the 828 cement used for attaching all the strain gauges to the model is adequate for its purpose, and that there is little likelihood that creep of the cement will have introduced significant errors*. However the thermal output does seem to be rather variable and, in view of the low magnitude of the measured thermal strains, this could have a very considerable effect on the accuracy of some of the calculated thermal stresses.

These investigations have not, of course, provided an explanation of the large overnight shift in the zero readings of the gauges used on the model. It may be seen, however, that there is no reason to question the suitability of the gauges and cement which were selected. It was eventually decided to accept the readings obtained during the heating up phase of the thermal stress test as being valid, subject to the reservation already mentioned regarding the variability of the thermal output. As noted in 3.3.1 the measured thermal strains were in general low and it was not felt that further work to elucidate the peculiar overnight shift would be justified.

---

* Subsequent to the completion of this investigation some work has been done by Hawker Siddeley Dynamics Ltd., under a Ministry of Technology Contract[4], to investigate further the thermal output and drift characteristics of the gauge/cement combination used here.

Appendix C

STRESSES IN THIN CYLINDERS WITH VARIOUS END RESTRAINTS

Ref.3 shows how, considering both membrane stresses and bending stresses, the equilibrium and compatibility equations for a closed circular cylindrical shell subjected to an internal pressure approximately reduce to

$$\frac{d^4w}{dx^4} + 4\beta^4 w = -\frac{p}{D} \tag{1}$$

where p = internal pressure

x = distance in the direction of the cylinder axis (see Fig.20)

w = displacement in the z direction

$D = Et^3/12(1 - \nu^2)$, the flexural ridigity of the shell (2)

$\beta^4 = Et/4D\,a^2 = 3(1 - \nu^2)/a^2\,t^2$ (3)

a = radius of the cylinder

t = wall thickness of the cylinder.

In the derivation of equation (1) the membrane stress resultant* in the x direction, N_x, is taken as zero and to obtain the complete stress situation it will be necessary to add on the direct stress in this longitudinal direction which is given by elementary shell theory as

$$\sigma_{\ell d} = \frac{pa}{2t} \quad . \tag{4}$$

The complete solution of equation (1) may be shown[3] to be

$$w = A_1 \sin\beta x \sinh\beta x + A_2 \sin\beta x \cosh\beta x + A_3 \cos\beta x \sinh\beta x + A_4 \cos\beta x \cosh\beta x - pa^2/Et \quad . \tag{5}$$

In the above equation A_1 to A_4 are arbitrary constants, which are determined by the boundary conditions of the problem. Having thus determined w, the required stress resultants are obtained by differentiation as follows

$$M_x = -D\frac{d^2w}{dx^2} \tag{6}$$

$$M_\phi = \nu M_x \tag{7}$$

---

*Stress resultants are forces or moments per unit length of side on which they act.

$$N_x = C \tag{8}$$

$$N_\phi = - Et \frac{w}{a} + \nu C \tag{9}$$

$$Q_x = - D \frac{d^3 w}{dx^3} \quad . \tag{10}$$

By choosing the origin at 0, as shown in Fig.20, conditions of symmetry demand that the radial deflections w have identical values at $\pm x$. Thus to ensure that only symmetrical terms are present both A_2 and A_3 must be zero. Equation (5) then reduces to

$$w = A_1 \sin \beta x \sinh \beta x + A_4 \cos \beta x \cosh \beta x - \frac{pa^2}{Et} \quad . \tag{11}$$

Three sets of end conditions will be considered for this symmetrical case.

C.1 Both ends free

For this situation the boundary conditions are

$$M_x = - D \frac{d^2 w}{dx^2} \text{ is zero at } x = \pm \frac{L}{2}$$

and

$$Q_x = - D \frac{d^3 w}{dx^3} \text{ is zero at } x = \pm \frac{L}{2} \quad ,$$

where L is the length of the cylinder.

Thus, writing $\beta L/2$ as α, and putting M_x and $Q_x = 0$ we have

$$A_1 \cos \alpha \cosh \alpha = A_4 \sin \alpha \sinh \alpha$$

and

$$(A_1 + A_4) \sin \alpha \cosh \alpha = (A_1 - A_4) \cos \alpha \sinh \alpha \quad .$$

For the above equations to be satisfied it is necessary that $A_1 = A_4 = 0$ and clearly the stress situation will be the simple membrane condition

$$M_x = M_\phi = Q_x = 0 \tag{12}$$

$$N_x = \frac{pa}{2} \quad \text{or} \quad \sigma_\ell = \frac{N_x}{t} = \frac{pa}{2t} \tag{13}$$

$$N_\phi = pa \quad \text{or} \quad \sigma_c = \frac{N_\phi}{t} = \frac{pa}{t} \; . \tag{14}$$

C.2 Both ends constrained against radial movement but allowed to rotate

For this situation the boundary conditions are

$$w = 0 \text{ and } \frac{d^2w}{dx^2} = 0 \text{ at } x = \pm \frac{L}{2} \text{ giving}$$

$$A_1 = \frac{pa^2}{Et}\left[\frac{\sin\alpha \sinh\alpha}{\sin^2\alpha \sinh^2\alpha + \cos^2\alpha \cosh^2\alpha}\right] \tag{15}$$

$$A_4 = \frac{pa^2}{Et}\left[\frac{\cos\alpha \cosh\alpha}{\sin^2\alpha \sinh^2\alpha + \cos^2\alpha \cosh^2\alpha}\right] \; . \tag{16}$$

The stress resultants then become

$$M_x = -2D\beta^2\left[A_1 \cos\beta x \cosh\beta x - A_4 \sin\beta x \sinh\beta x\right] \tag{17}$$

$$M_\phi = \nu M_x \tag{18}$$

$$N_x = \frac{pa}{2} \tag{19}$$

$$N_\phi = -Et\,\frac{\left[A_1 \sin\beta x \sinh\beta x + A_4 \cos\beta x \cosh\beta x\right]}{a} + pa \tag{20}$$

$$Q_x = -2D\beta^3\left[-(A_1 + A_4)\sin\beta x \cosh x + (A_1 - A_4)\cos\beta x \sinh\beta x\right] \; . \tag{21}$$

C.3 Both ends supported by rigid end plates

For this situation the boundary conditions are

$$w = 0 \text{ and } \frac{dw}{dx} = 0 \text{ at } x = \pm \frac{L}{2} \; .$$

It may be shown that under these conditions

$$A_1 = \frac{2pa^2}{Et}\left[\frac{\sin\alpha\,\cosh\alpha - \cos\alpha\,\sinh\alpha}{\sin 2\alpha + \sin 2\alpha}\right]$$

$$A_4 = \frac{2pa^2}{Et}\left[\frac{\cos\alpha\,\sinh\alpha + \sin\alpha\,\cosh\alpha}{\sin 2\alpha + \sinh 2\alpha}\right] .$$

The stress resultants are again, given by equations (17) to (21).

Table 1

TEMPERATURE DISTRIBUTION

Thermo-couple No.	Position	Prototype			Model	
		T °C	T = T-330	$\frac{1}{2}\Delta T$	T °C	Measured $\frac{1}{2}\Delta T$
1.1	At 135° to cylinder centre-lines, on sphere	440	110	55	108	56
1.2	Top of sphere on vertical	490	160	80	132	80
1.3	At 45° to cylinder centre-lines, on sphere	330	0	0	52	0
1.4	Bottom of sphere on vertical	360	30	15	67	15
2.1	Top of small cylinder	480	150	75	124	72
2.2	Bottom of small cylinder	500	170	85	137	85
2.3	Top of large cylinder	450	120	60	110	58
2.4	Bottom of large cylinder	450	120	60	114	62

Table 2

THERMAL STRESS TEST

Stresses are calculated assuming $E = 30 \times 10^6$ lbf/in^2 and $\nu = 0.28$

Gauge No.	Gauge position	Orientation	με	σ lbf/in^2	σ kN/m^2	Comments
14	1BE	⊥ plane of the cylinders	204	6900	47000	
9	1TE	$\|\|^{\ell}$ plane of the cylinders	24	2600	18000	
-	1BI	⊥ plane of the cylinders	-	-	-	Not gauged
-	1TI	$\|\|^{\ell}$ plane of the cylinders	-	-	-	Not gauged
-	2BE	⊥ axis of the large cylinder	-	-		Gauge failed
10	2TE	$\|\|^{\ell}$ axis of the large cylinder	34	-		Gauge failed
5	2BI	⊥ axis of the large cylinder	126	4900	34000	
1	2TI	$\|\|^{\ell}$ axis of the large cylinder	86	3900	27000	
15	3BE	Circumferential	78	2100	14500	
11	3TE	Longitudinal	-48	-900	-6000	
6	3BI	Circumferential	90	2600	18000	
2	3TI	Longitudinal	-36	-400	-3500	
16	4BE	Circumferential	2	1100	7600	
12	4TE	Longitudinal	116	4000	27500	
-	4BI	Circumferential			-	Not gauged
-	4TI	Longitudinal				Not gauged
17	5BE	Circumferential	-66	-1700	-12000	
13	5TE	Longitudinal	50	1000	7000	
7	5BI	Circumferential	110	4900	34000	
3	5TI	Longitudinal	146	5800	40000	
18	6BE	$\|\|^{\ell}$ plane of the cylinders	-18	-	-	
19	6TE	⊥ plane of the cylinders	-	-	-	Gauge failed.*
8	6BI	$\|\|^{\ell}$ plane of the cylinders	-68	-5200	-36000	
4	6TI	⊥ plane of the cylinders	-328	-11300	-78000	

Identification of gauge position

1 - 6 gives the position on the model.

B or T meaning bottom or top indicates the relative positions of the two gauges at a particular point.

E or I signifies external or internal.

NOTE:- Only half the required temperature differences could conveniently be applied and the results obtained were doubled to give the above table.

* Replaced for pressure test.

Table 3

INTERNAL PRESSURE TESTS

Gauge No.	Gauge position	Test 1 thick seal		Test 2 thin seal		Comments
		με	σ/p	με	σ/p	
14	1BE	248	13.9	248	13.7	
9	1TE	252	13.9	248	13.7	
-	1BI	-	-	-	-	Not gauged
-	1TI	-	-	-	-	Not gauged
-	2BE	-	-	-	-	Gauge failed during wiring
10	2TE	189	-	187	-	
5	2BI	-	-	-	-	Gauge failed during wiring
1	2TI	315	-	29	-	
15	3BE	874	37.6	480	22.2	
11	3TE	-22	9.6	102	10.3	
6	3BI	855	33.2 (33.6)[3]	855	33.0 (33.8)	See note (2) below
2	3TI	-324 (-292)	-3.7 (-2.3)	-346 (-270)	-4.7 (-1.3)	
16	4BE	1059	45.7	650	29.8	
12	4TE	-17	12.1	141	14.0	
-	4BI	-	-	-	-	Not gauged
-	4TI	-	-	-	-	Not gauged
17	5BE	985	45.6	660	31.4	
13	5TE	240	22.2	238	18.4	
7	5BI	-339	-22.0 (-18.0)	-334	-22.2 (-17.3)	
3	5TI	-595 (-273)	-29.8 (-16.0)	-641 (-239)	-31.8 (-14.4)	
18	6BE	426	18.8	416	18.7	
19	6TE	25	6.3	50	7.2	
8	6BI	403	25.0	-634	-33.6	
4	6TI	624	32.0	-501	-29.4	

Applied internal pressure = 750 lbf/in^2 (5170 kN/m^2)

Notes: (1) It is possible that high strain gradients were present at positions (3), (4), (5) and (6); thus the validity of the calculated stresses must be questionable (see section 3.4.1, paragraph 5).

(2) Results for gauge 6 are taken from a trial run after which this gauge became unreliable.

(3) Values in brackets assume linearity throughout (see section 3.4.1, paragraph 3).

Table 4

A COMPARISON OF MEASURED AND THEORETICALLY PREDICTED STRAINS

Gauge position (5)

Boundary condition		Gauge orientation	Surface strain (με)	
No.	Description		External	Internal
1	Completely free	Circumferential	360	360
		Longitudinal	90	90
2	Ends free to rotate only	Circumferential	75	75
		Longitudinal	365	30
3	Ends built-in	Circumferential	-25	-25
		Longitudinal	90	315
-	Measured values Test 1	Circumferential	985	-340
		Longitudinal	240	-275
-	Test 2	Circumferential	660	-335
		Longitudinal	240	-240

Gauge position (3)

Boundary condition		Gauge orientation	Surface strain (με)	
No.	Description		External	Internal
1	Completely free	Circumferential	360	360
		Longitudinal	90	90
2	Ends free to rotate only	Circumferential	280	280
		Longitudinal	400	-160
3	Ends built-in	Circumferential	85	85
		Longitudinal	435	-110
-	Measured values Test 1	Circumferential	875	855
		Longitudinal	-20	-290
-	Test 2	Circumferential	480	855
		Longitudinal	100	-270

Note: The measured values are subject to the restrictions listed as comments in Table 3.

Table 5

COMPARISON OF CEMENT CHARACTERISTICS TEST A

Temp. °C	State of loading	Bridge reading $\delta R/R$ ($\mu\Omega/\Omega$)		$\Delta(\delta R/R)$ ($\mu\Omega/\Omega$)		Comments
		Gauge (1)	Gauge (2)	Gauge(1)	Gauge (2)	
24.5	U	0	0			Gauge (1) nearest encastré end
				2320	1925	
24.5	L	2320	1925			
				-2320	-1925	
24.5	U	0	0			
24.5	U	0	0			Gauge (2) nearest encastré end
				1910	2310	
24.5	L	1910	2310			
				-1910	-2310	
24.5	U	0	0			
				- 200	- 100	
90	U	- 200	- 100			
				2330	1915	
90	L	2130	1815			
				-2330	-1920	
90	U	- 200	- 105			
				- 120	- 15	
131	U	- 320	- 120			
				2360	1920	
131	L	2040	1800			
132	P.L.	780	810			Total time under load 0 hour
				- 10	- 20	
133	P.L.	770	790			Total time under load ½ hour
				- 10	- 0	
129	P.L.	760	790			Total time under load 1 hour
				0	0	
130	P.L.	760	790			Total time under load 1½ hours

U = unloaded
L = loaded
P.L. = partially loaded

Gauge (1) cemented with 828 + M
Gauge (2) cemented with BR 600

Table 6

COMPARISON OF CEMENT CHARACTERISTICS TEST B

Temp. °C	State of loading	Bridge reading $\delta R/R$ ($\mu\Omega/\Omega$)		$\Delta(\delta R/R)$ ($\mu\Omega/\Omega$)		Comments
		Gauge (3)	Gauge (4)	Gauge (3)	Gauge (4)	
24	U	-1500	0			Gauge (3) nearest encastré end
				2290	1900	
24	L	790	1900			
				-2290	-1900	
24	U	-1500	0			
24	U	-1500	5			Gauge (4) nearest encastré end
				1850	2270	
24	L	350	2275			
				-1850	-2260	
24	U	-1500	15			
				-175	-50	
130	U	-1675	-40			
				1825	2260	
130	L	150	2220			
				-1850	-2260	
128	U	-1700	-40			
135	U	-1700	-25			Gauge (3) nearest encastré end
				2395	1825	
134	L	695	1800			Total time under load 0 hour
				-175	-250	
135	L	520	1550			Total time under load $1\frac{1}{2}$ hours
				-20	-50	
135	L	500	1500			
				0	0	
139	L	500	1500			Total time under load $3\frac{1}{2}$ hours
				-2250	-1750	
137	U	-1750	-250			
				500	100	
25	U	-1250	-150			Reading taken the following morning

U = Unloaded
L = Loaded

Gauge (3) cemented with 828 + M
Gauge (4) cemented with BR 600

Table 7

A COMPARISON OF BRITTLE COATING AND STRAIN GAUGE RESULTS

Gauge position	Gauge No.	Isoentatic*	Surface strain	
			From brittle coating	From strain gauges
1BE	14	Less than green	< 400	240
1TE	9	Less than green	< 400	240
2BE	-	Less than green	< 400	-
3BE	15	Black	470	470
4BE	16	Green-black	440	570
5BE	17	Red	560	515
6BE	18	Brown	700	455

Applied internal pressure 800 lbf/in^2 (5520 kN/m^2) for brittle coating test

Applied internal pressure 750 lbf/in^2 (5175 kN/m^2) for brittle coating test

Threshold strain taken as 350 $\mu\varepsilon$

*Colour code for isoentatics

Applied pressure		Isoentatic colour
lbf/in^2	kN/m^2	
400	2760	Brown
500	3450	Red
600	4140	Black
700	7830	Yellow
800	5520	Green

REFERENCES

No.	Author	Title, etc.
1	G.N. Doyle	The design and testing of the cascade corner bend for the 66 in bore ducting for Trawsfynydd. Richardsons, Westgarth & Co. Ltd. Engineering Division Report A 36 (1960)
2	V.M. Hickson	Special techniques in experimental stress analysis. Experimental Mechanics, Pergamon Press (1963) R.A.E. Technical Note Structures 302 (A.R.C.23506)(1961)
3	J.E. Gibson	Linear elastic theory of thin shells. Pergamon Press (1965)
4	A.G. Goodwin	Investigation to establish drift and creep performance of Budd C6-124 strain gauges using Shell Epikote adhesive. Hawker Siddeley Dynamics Ltd., Environmental Engineering Department Report 152 (1969)

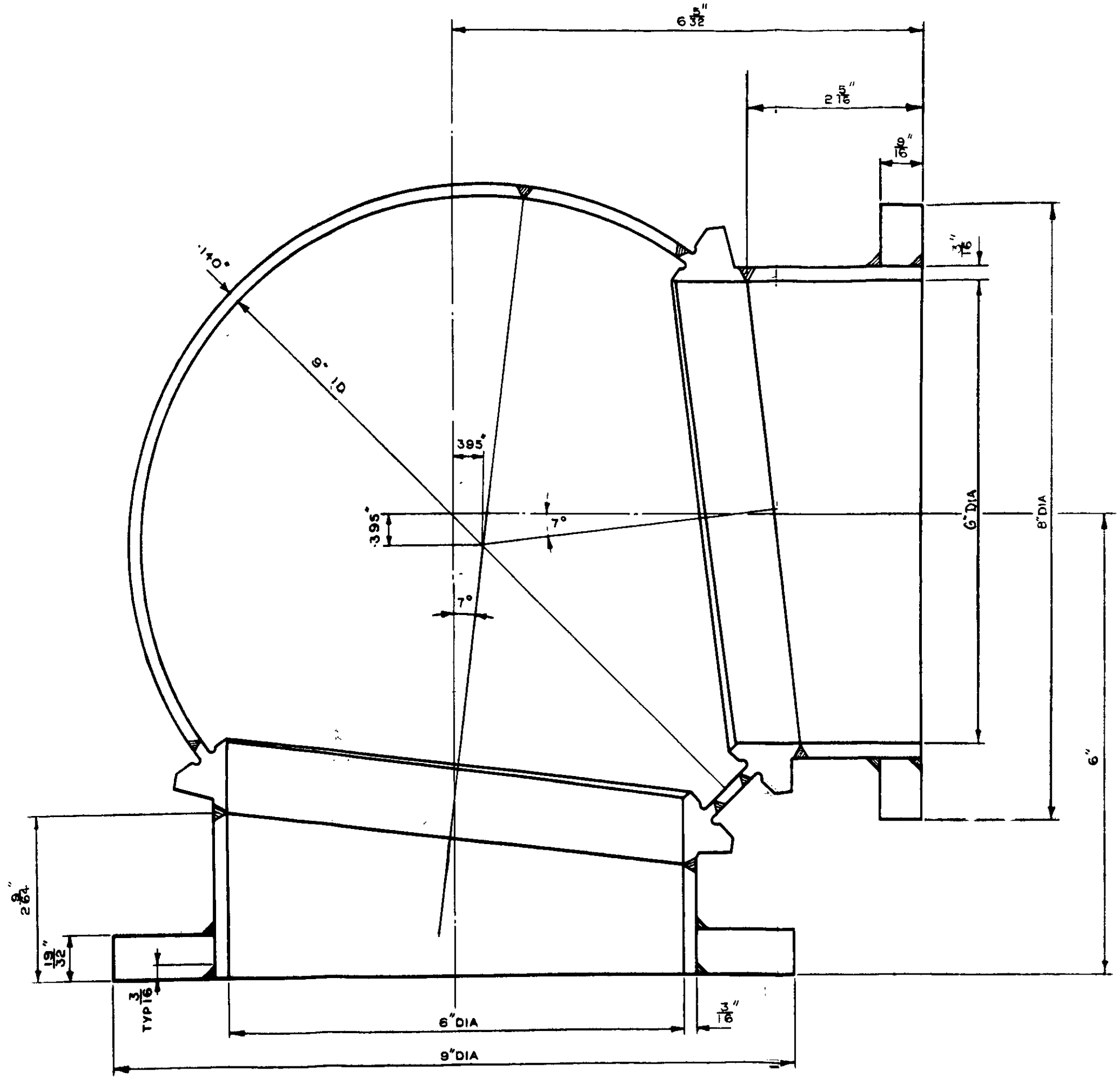

Fig. 1 Corner model

3RD angle projection

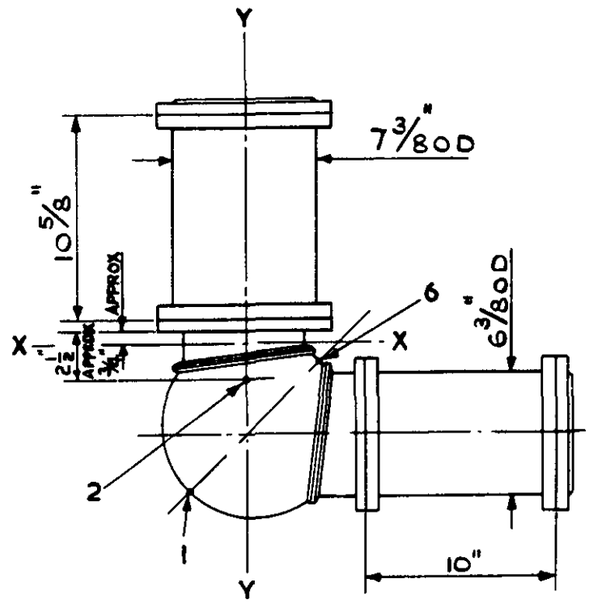

Horizontal plan

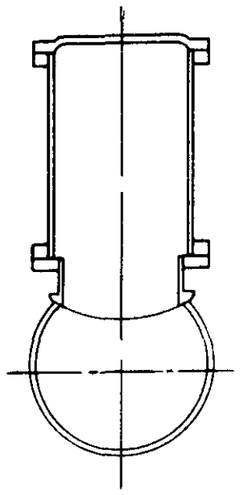

Section Y Y

Nos 1 to 6 indicate strain gauge positions

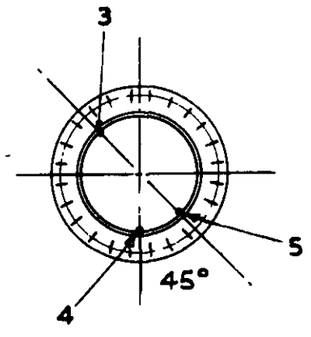

Section X X

Fig. 2 Model assembly and strain gauge location

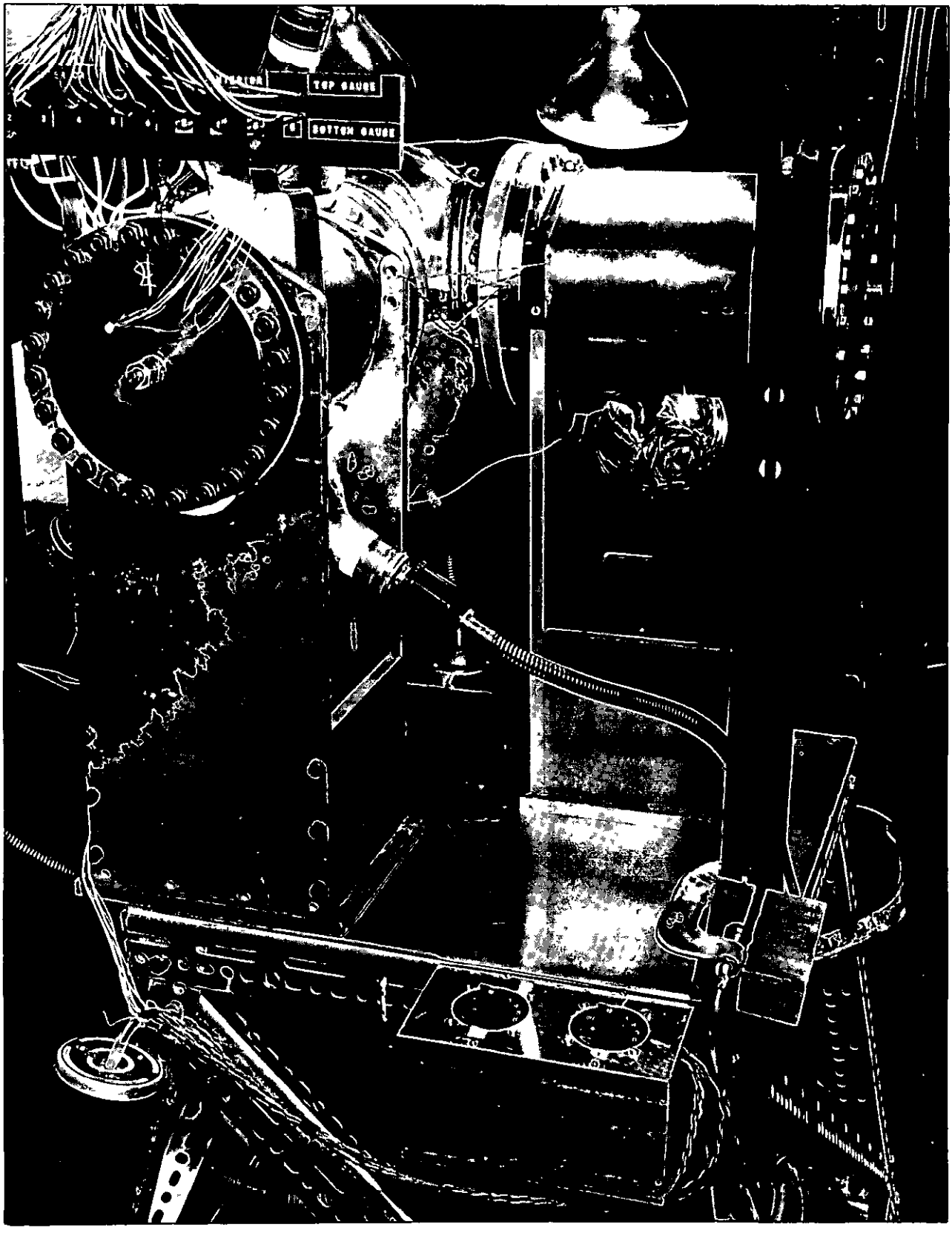

Fig.3 Heating and cooling system used for the thermal stress test

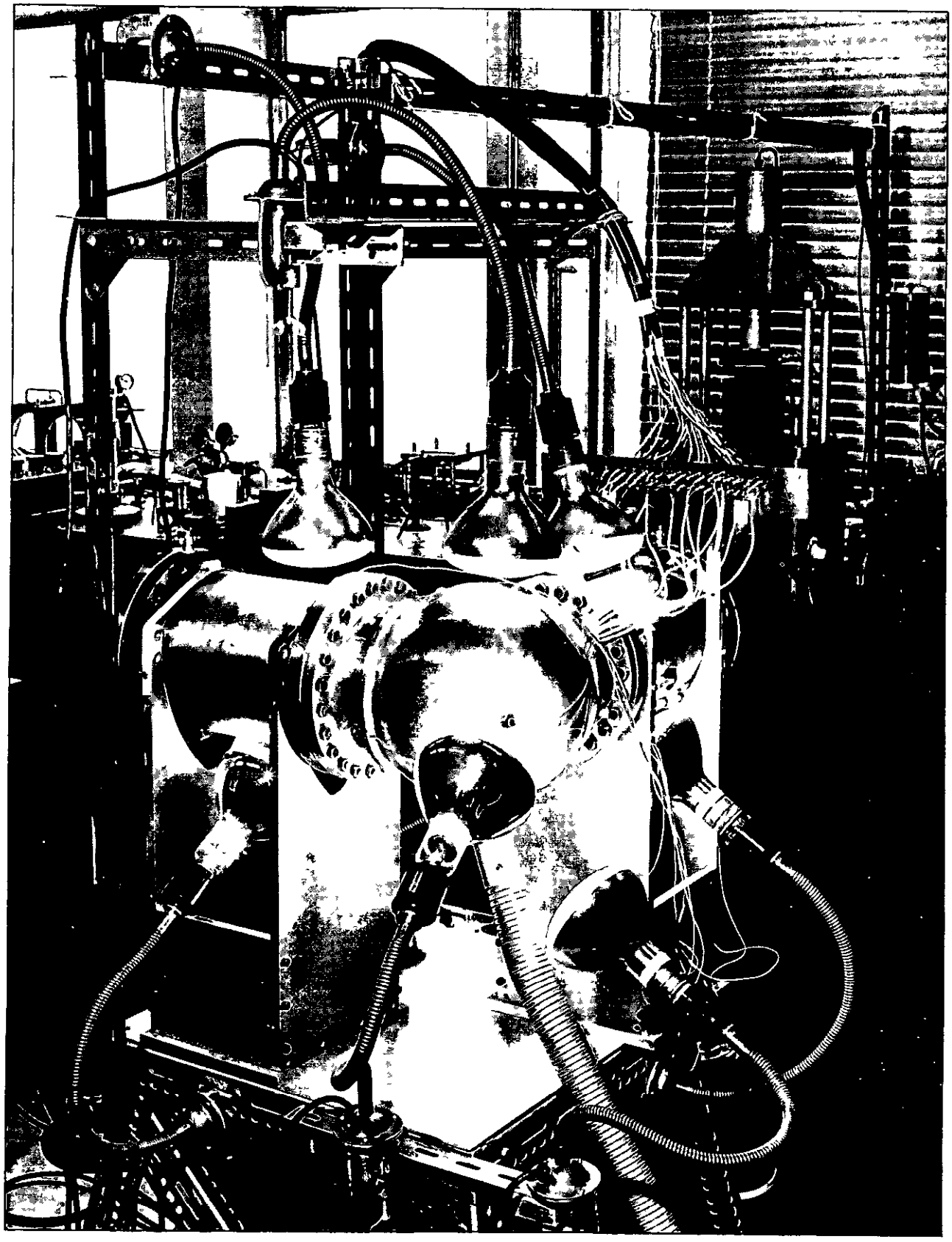

Fig.4 Heating and cooling system used for the thermal stress test

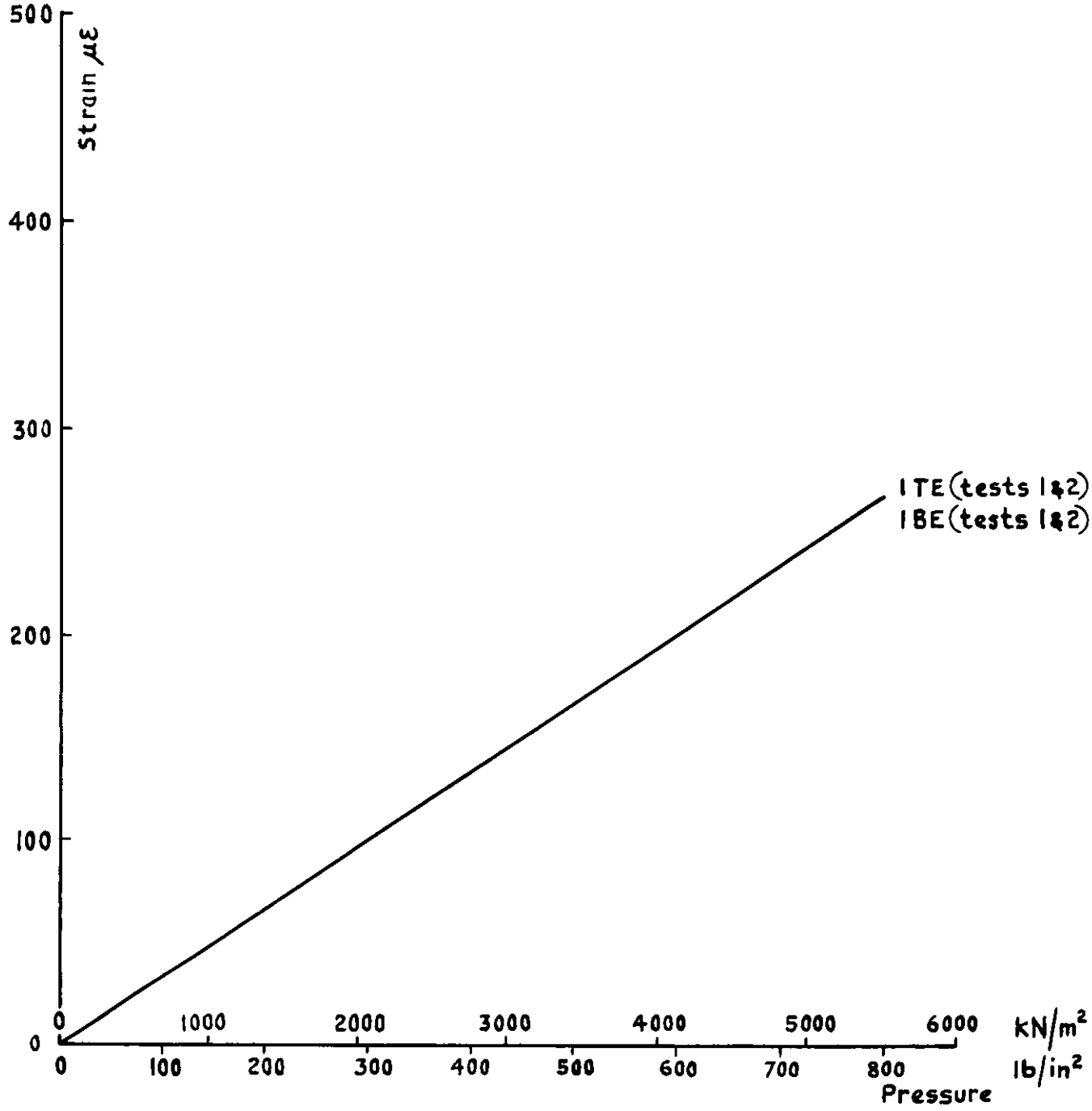

Fig.5 Internal pressure test
Strain gauge readings at position 1

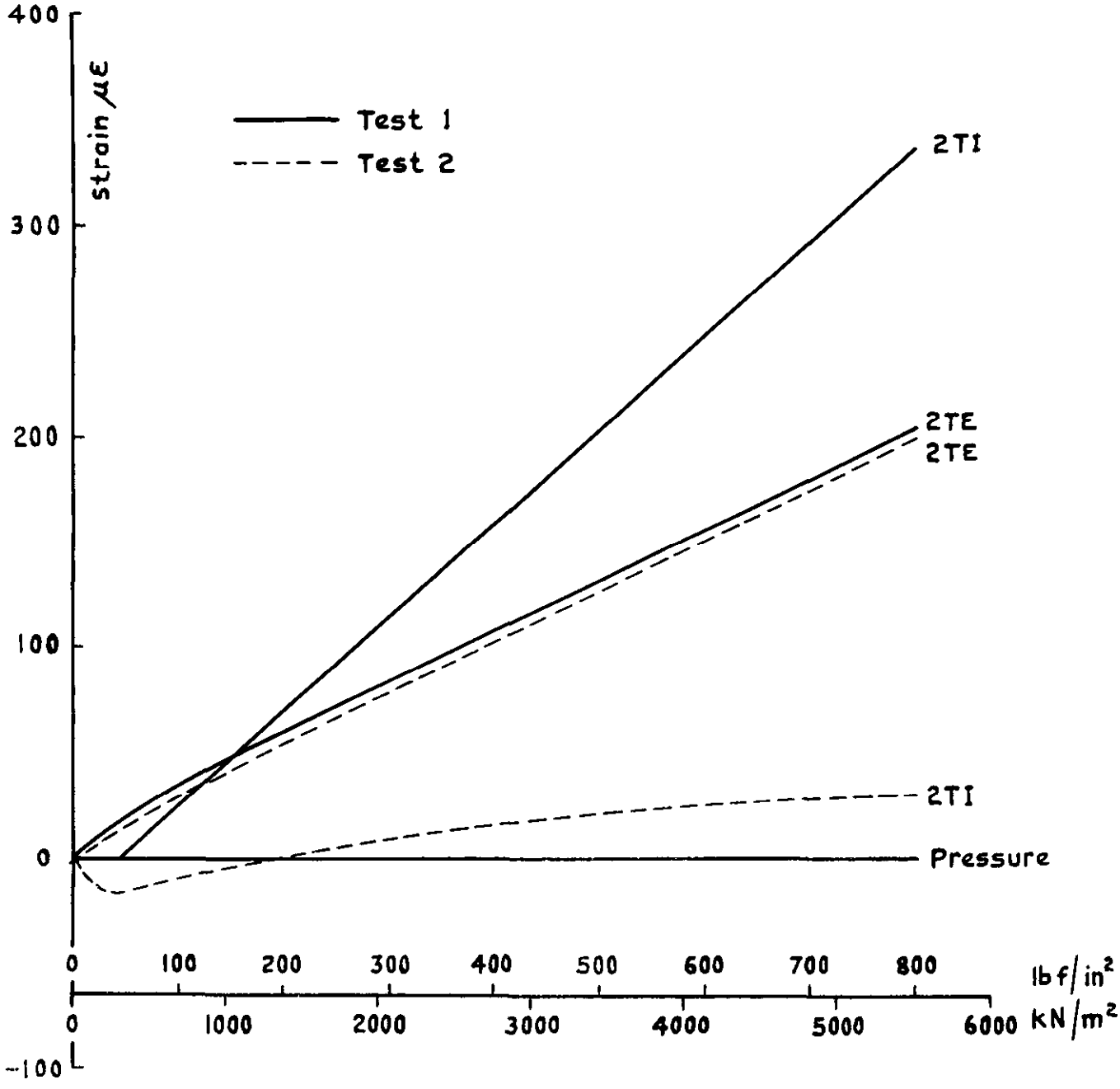

Fig.6 Internal pressure test
Strain gauge readings at position 2

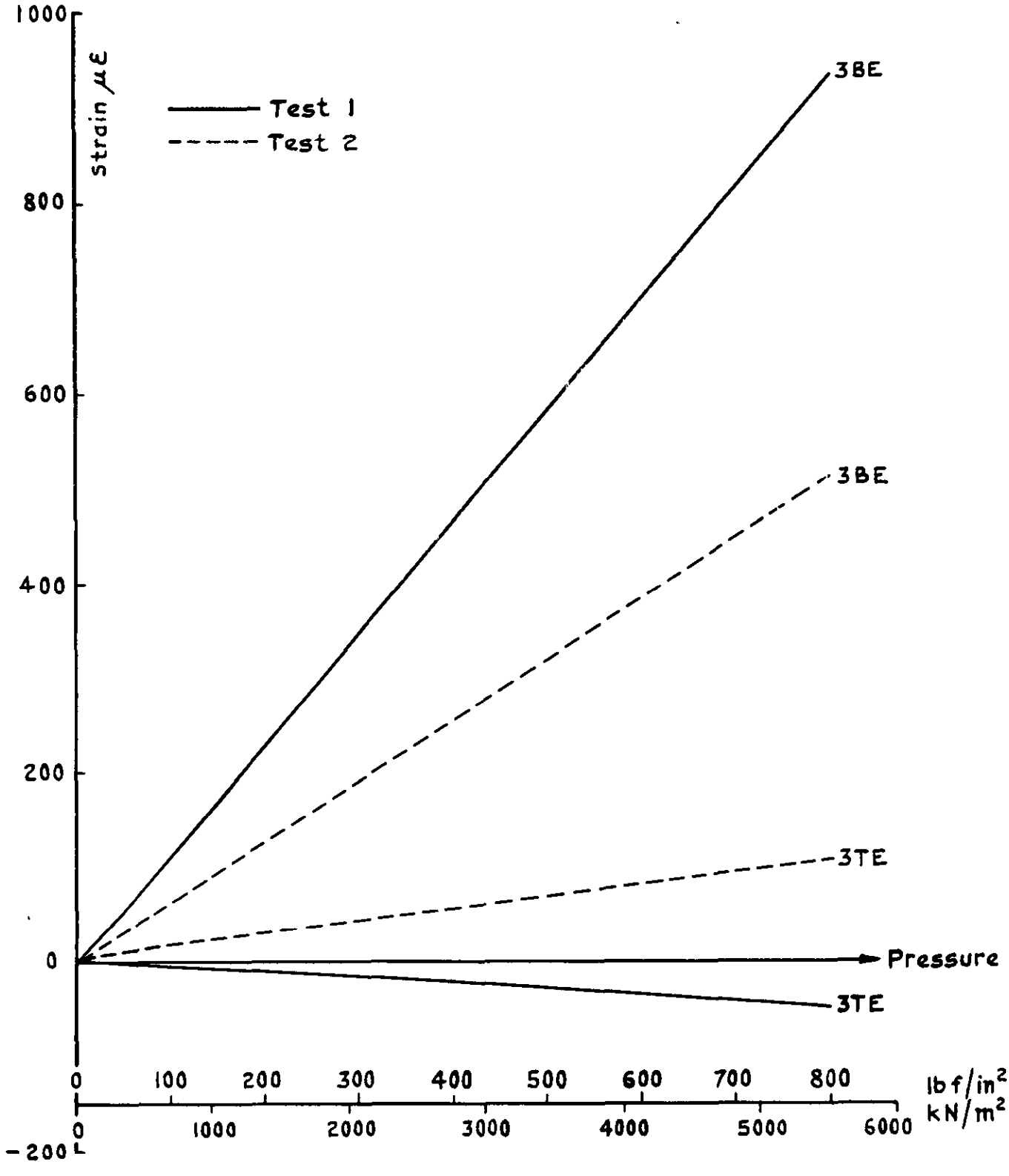

Fig. 7 Internal pressure test
External strain gauge readings at position 3

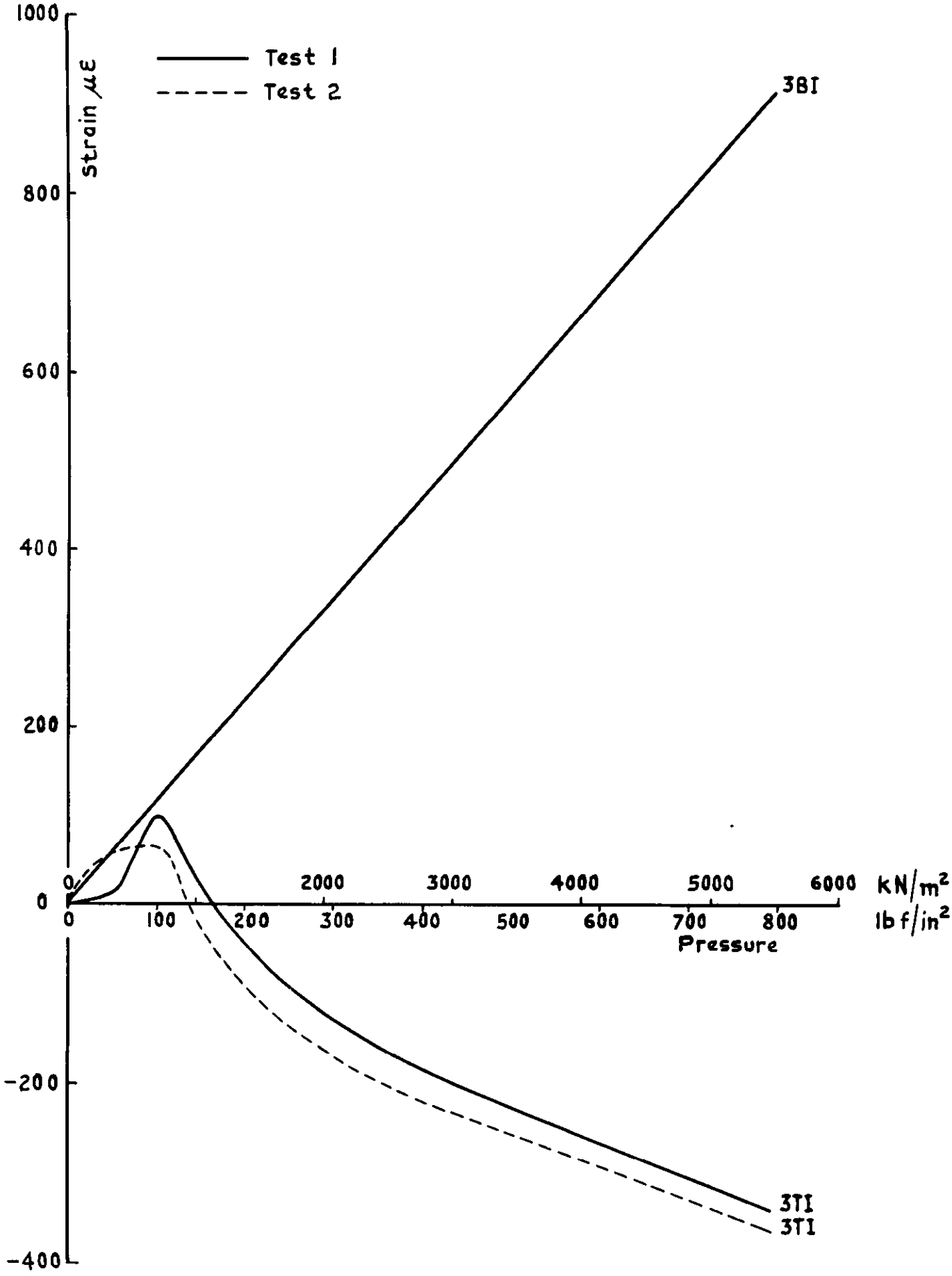

Fig.8 Internal pressure test
Internal strain gauge readings at position 3

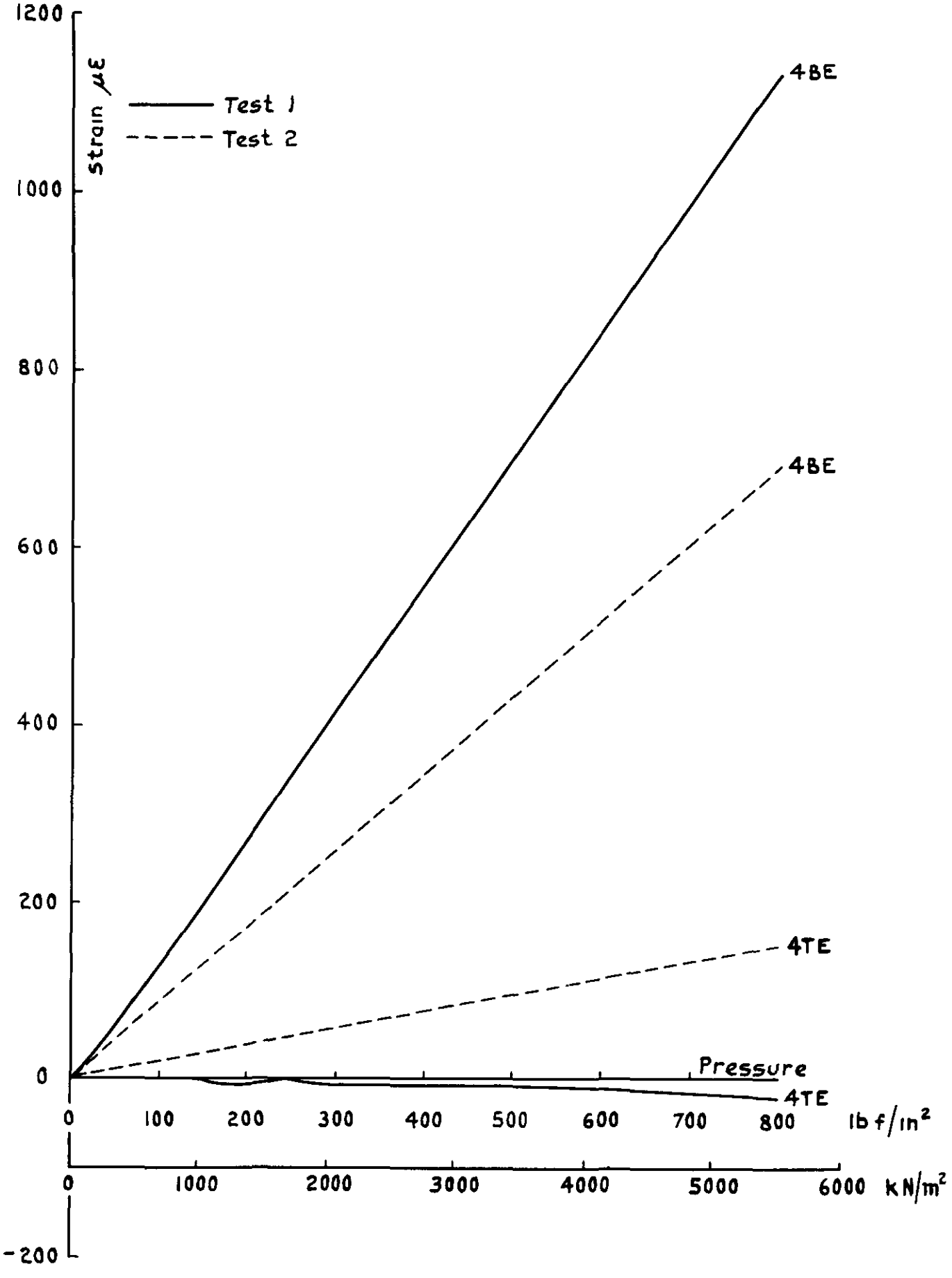

Fig. 9 Internal pressure test
Strain gauge readings at position 4

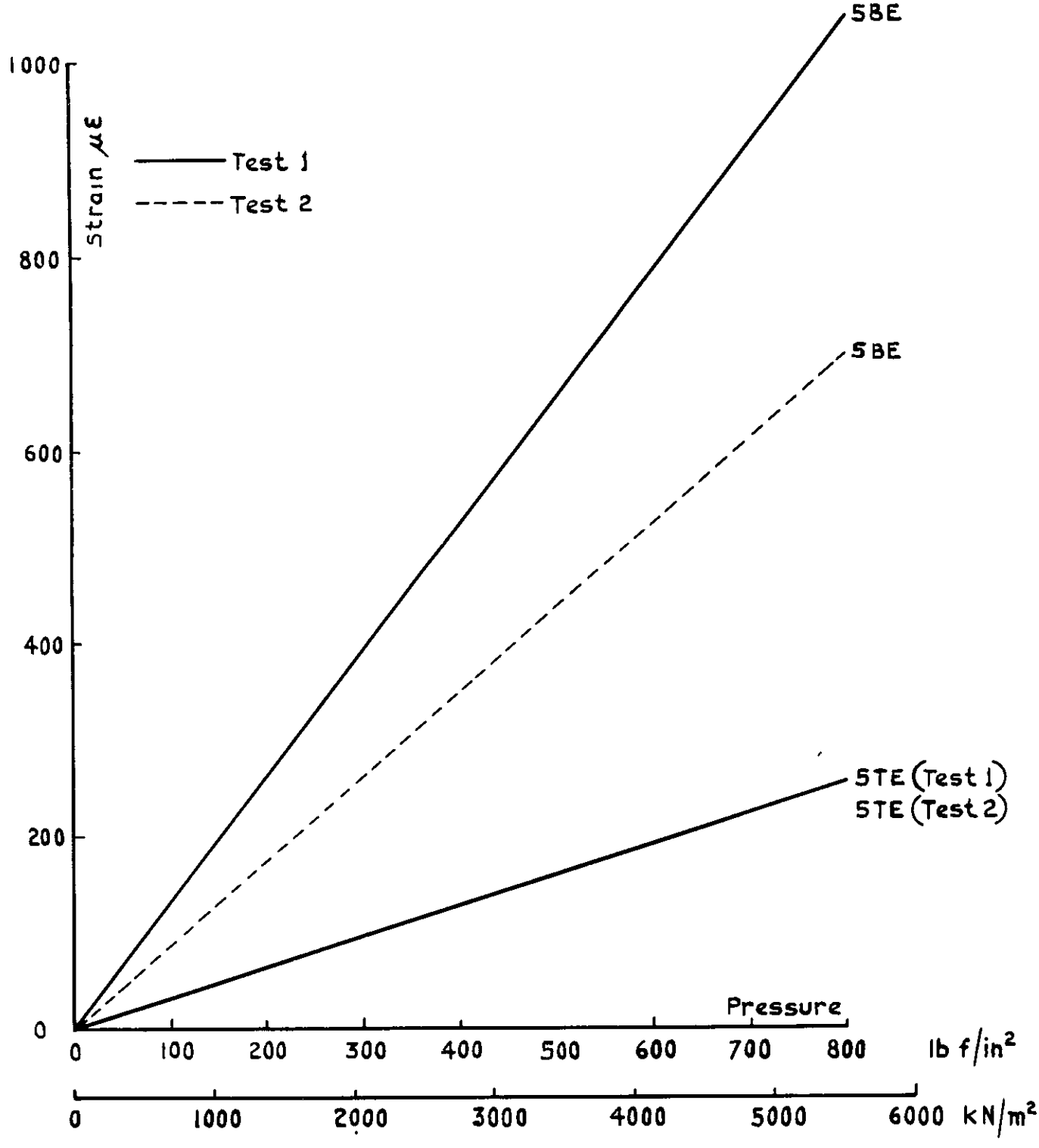

Fig. 10 Internal pressure test
External strain gauge readings at position 5

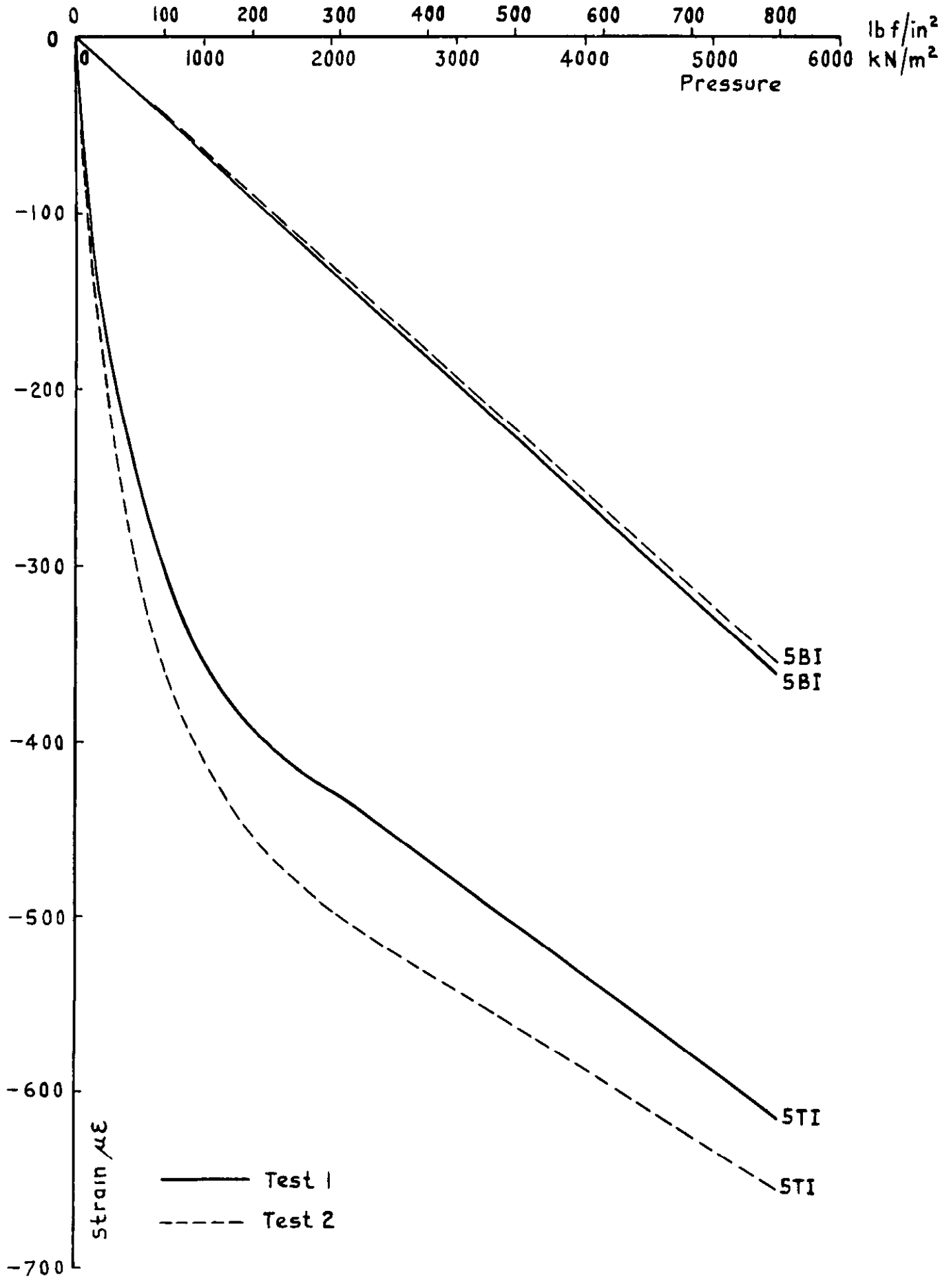

Fig. 11 Internal pressure test
Internal strain gauge readings at position 5

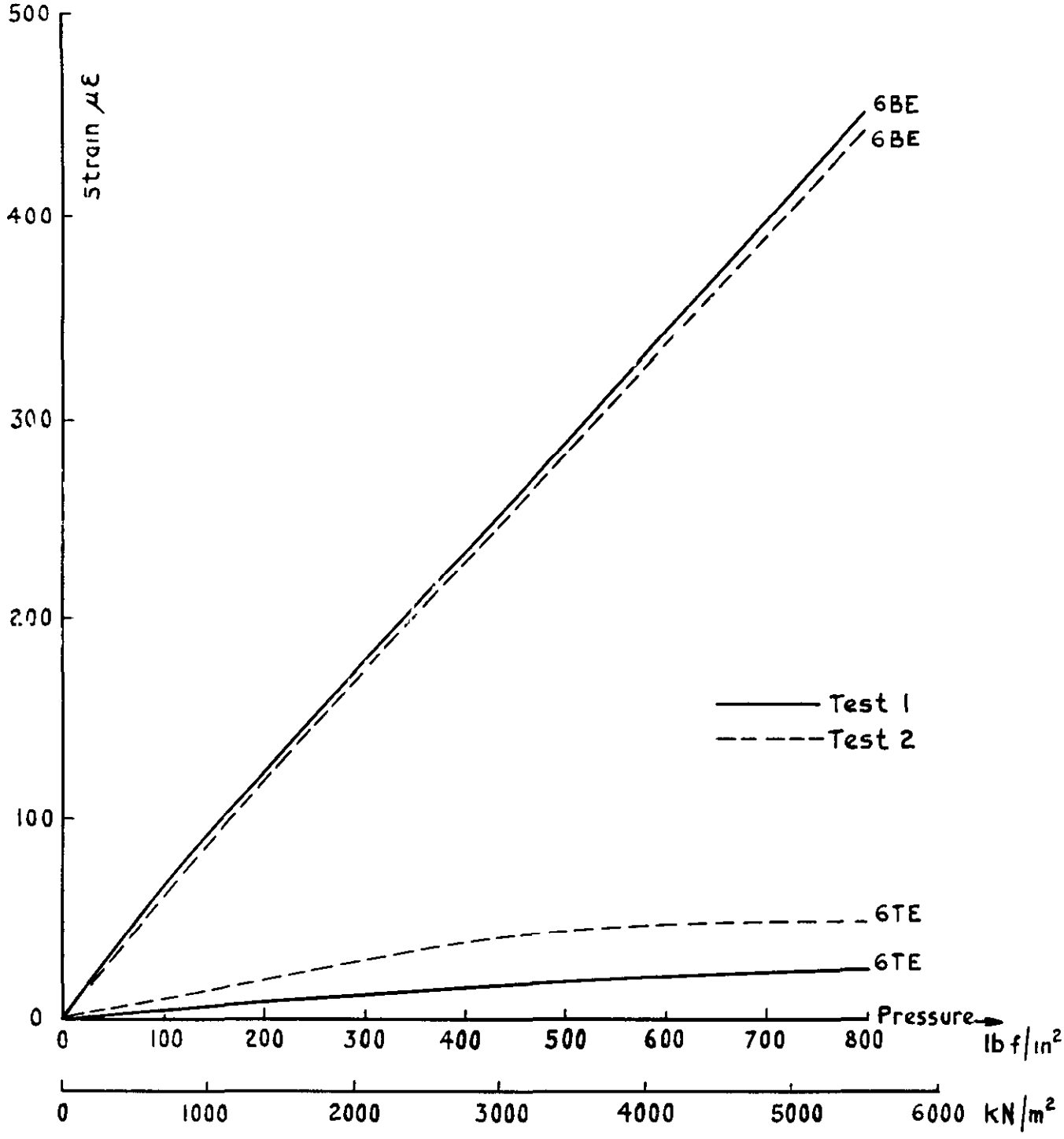

Fig.12 Internal pressure test
External strain gauge readings at position 6

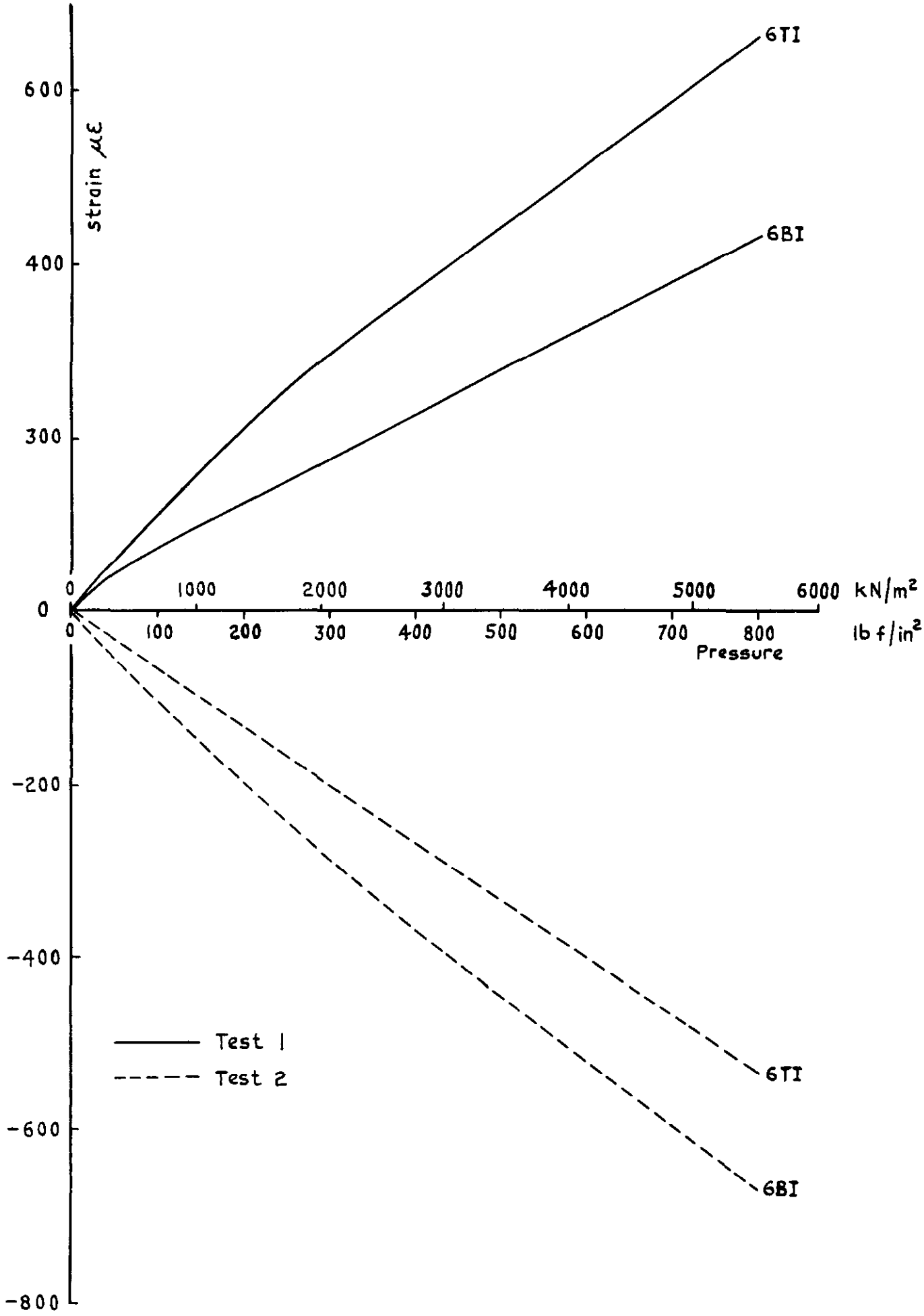

Fig.13 Internal pressure test
Internal strain gauge readings at position 6

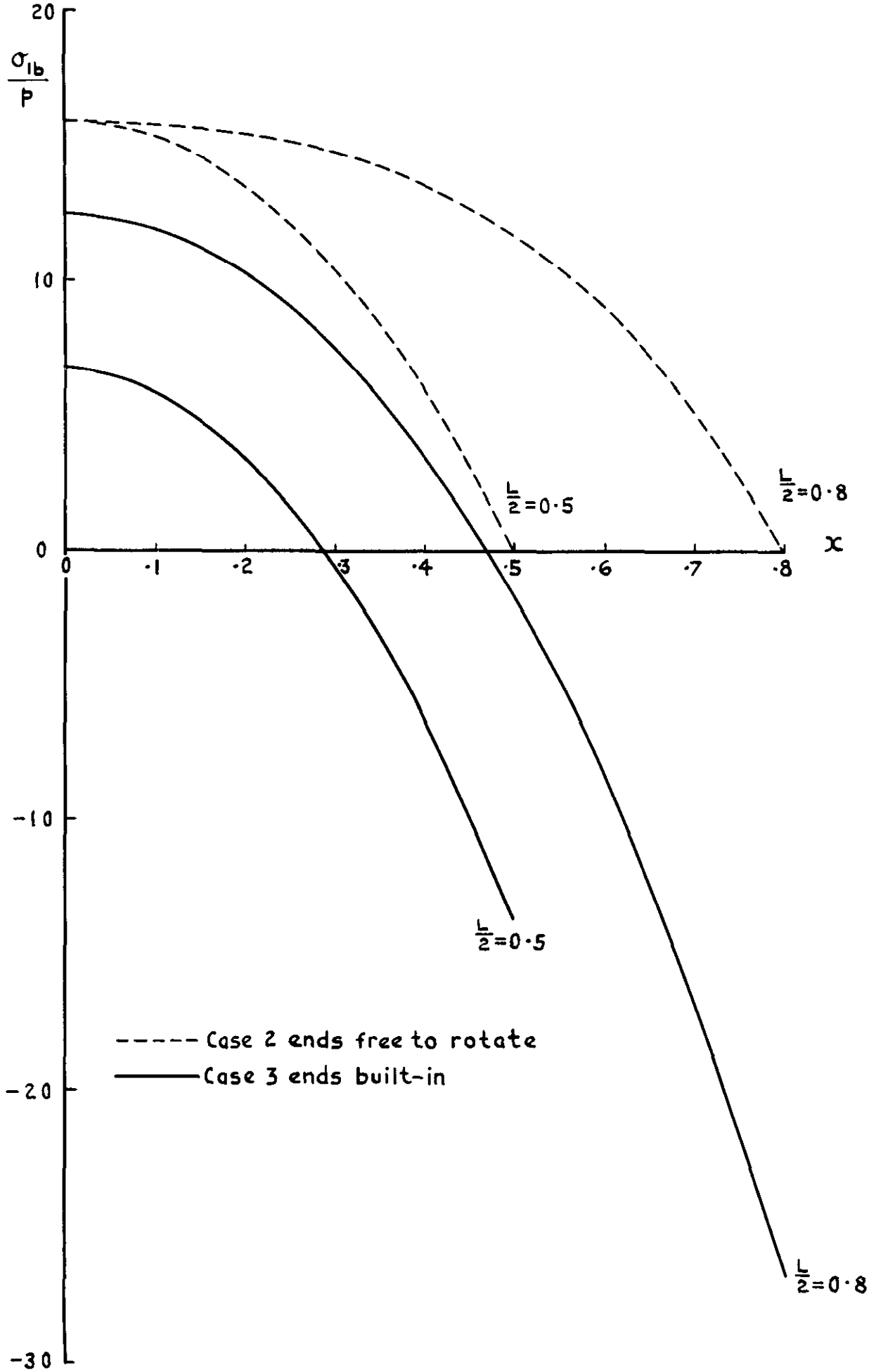

Fig. 14 Theoretically derived longitudinal bending stress

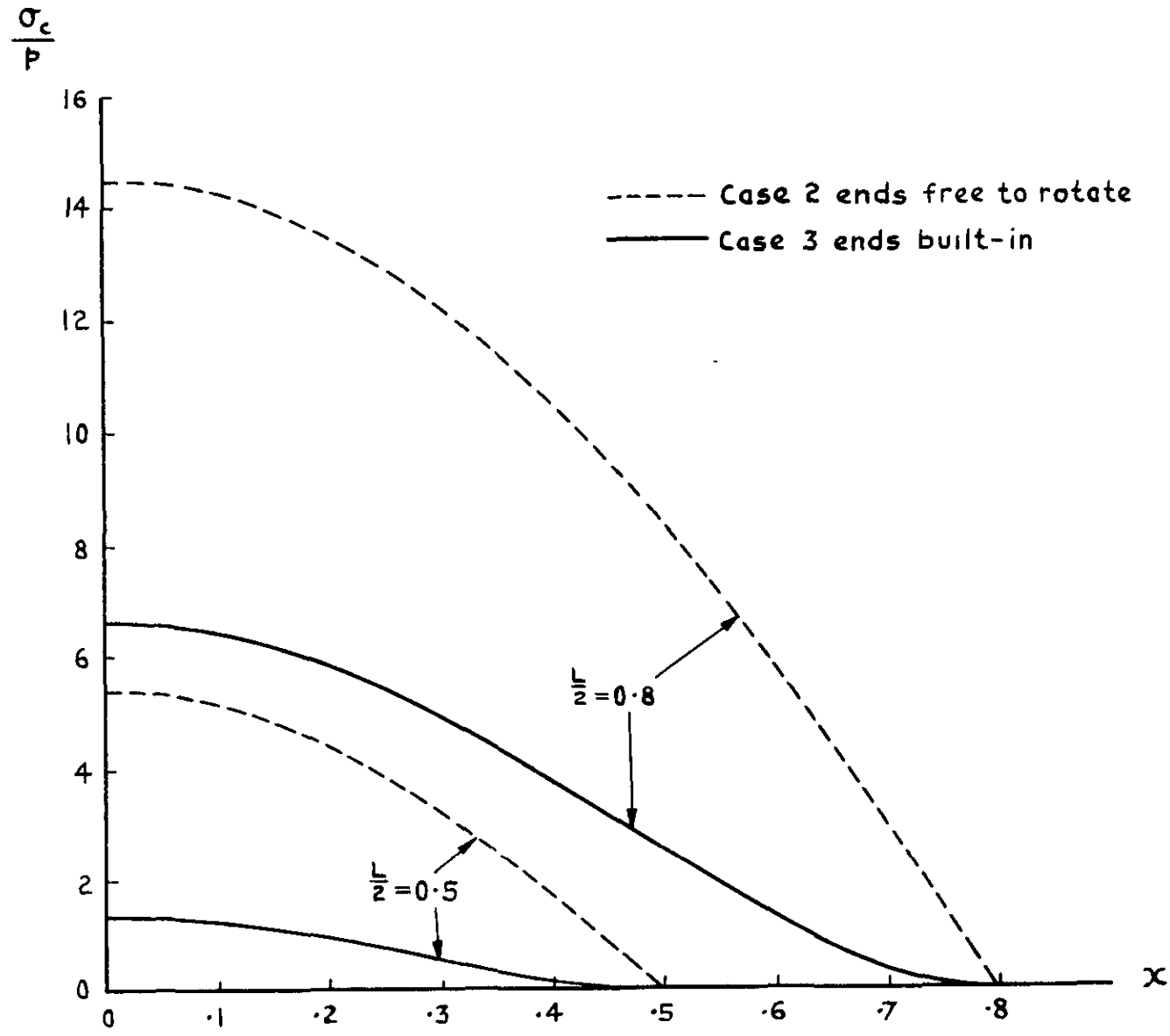

Fig. 15 Theoretically derived circumferential stress

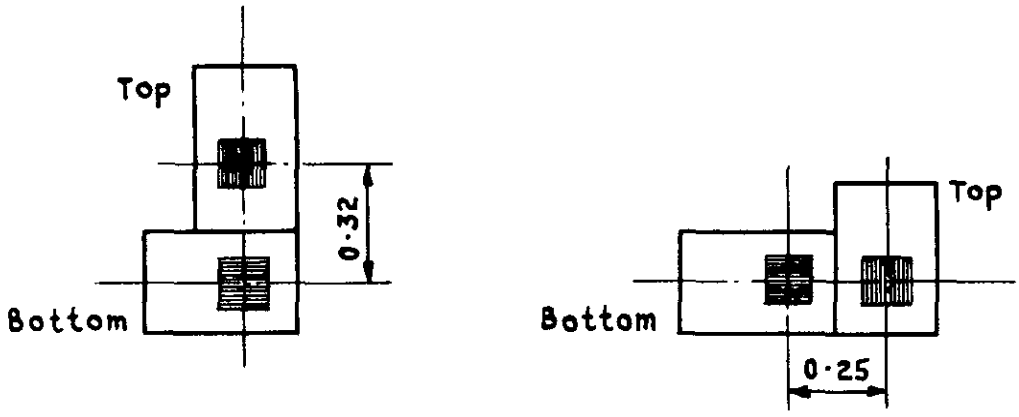

a Standard

b At position (6)

2 x full size

Fig.16 a & b Relative positions of top and bottom gauges

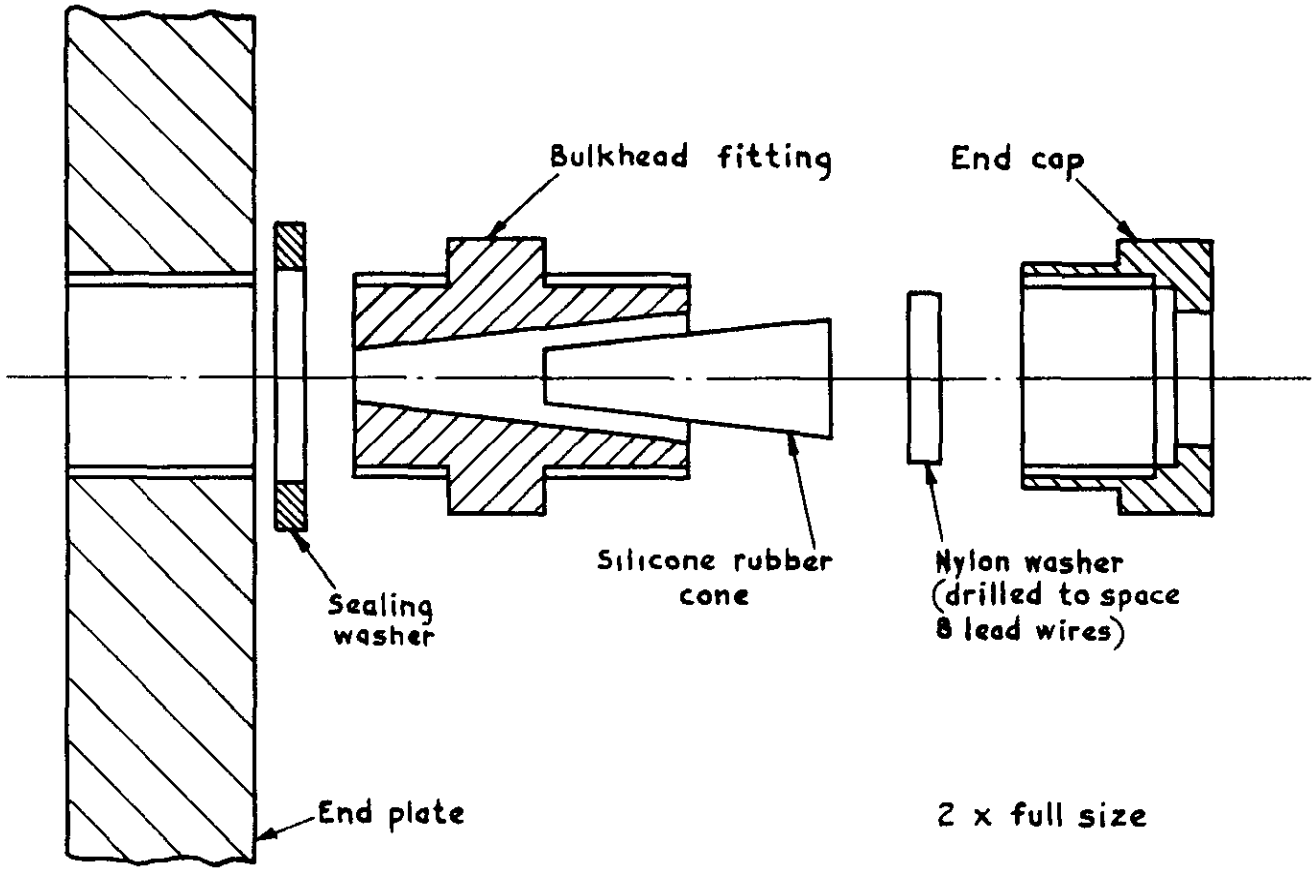

Fig.17 Bulkhead fitting

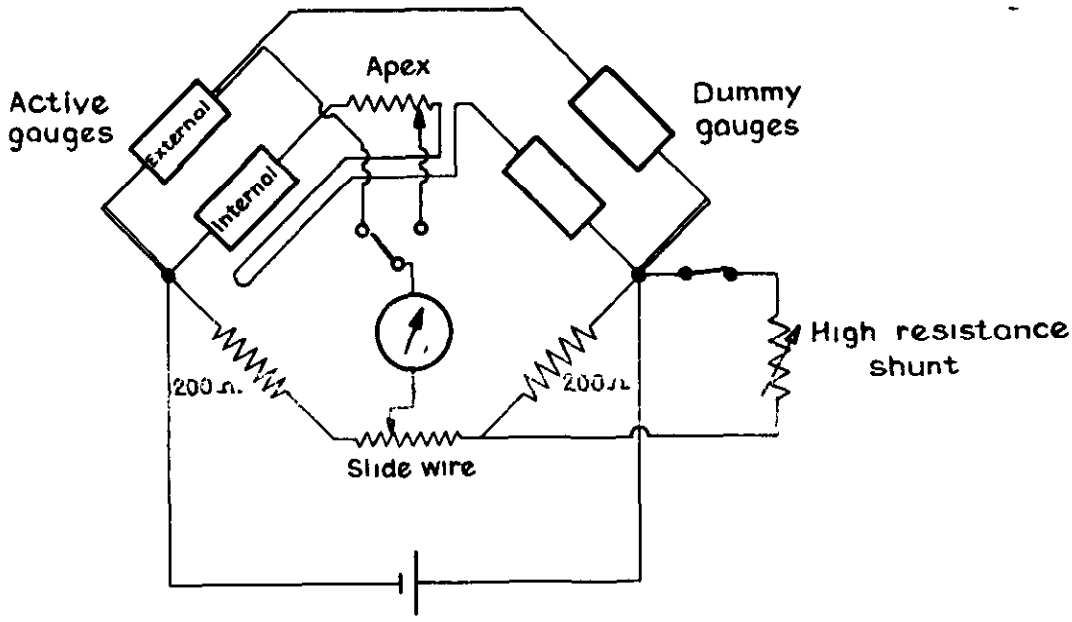

Bridge network showing 2 wire and 3 wire systems

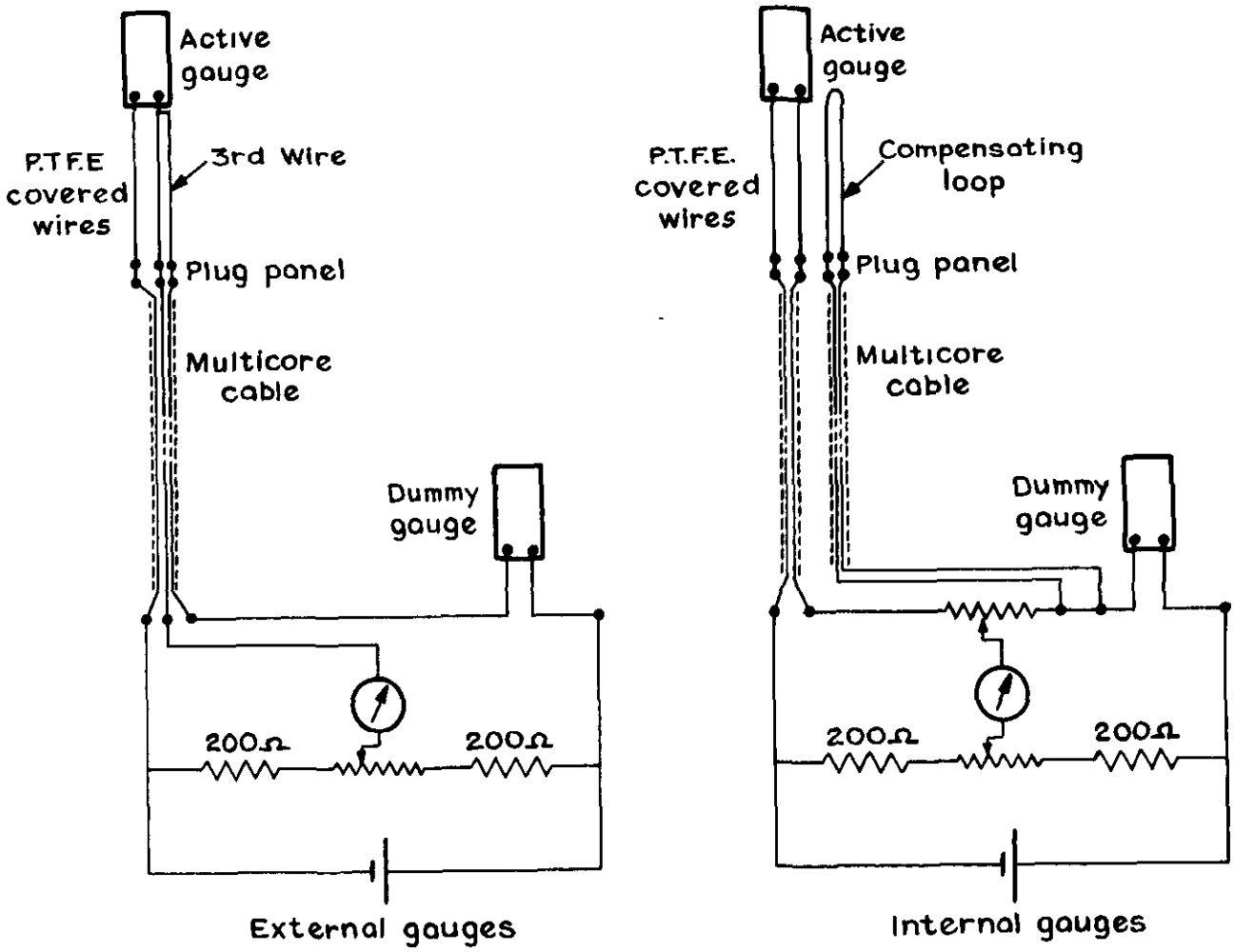

Physical layout of leads to obtain complete temperature compensation

Fig. 18 Strain gauge wiring diagrams

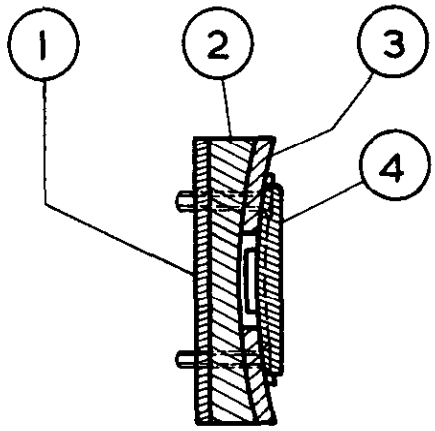

Section A A

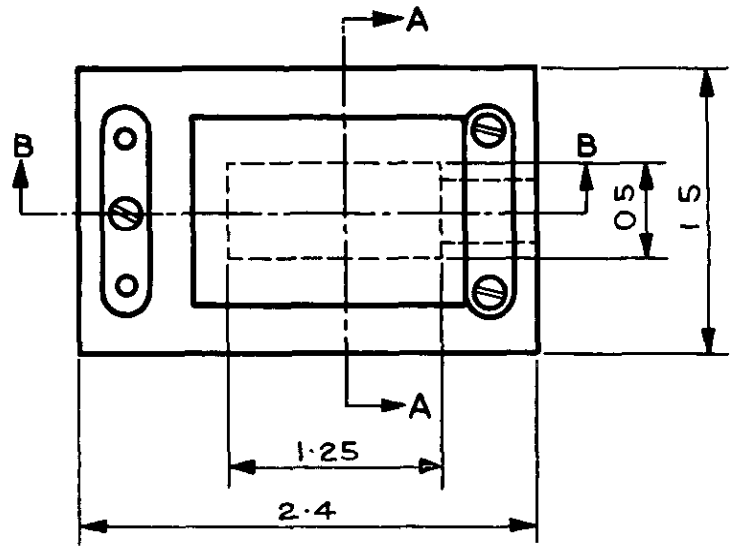

1 Base plate
2 Plaster mould
3 Silicone rubber
4 Cover plate
5 Clamps

Dimensions in inches

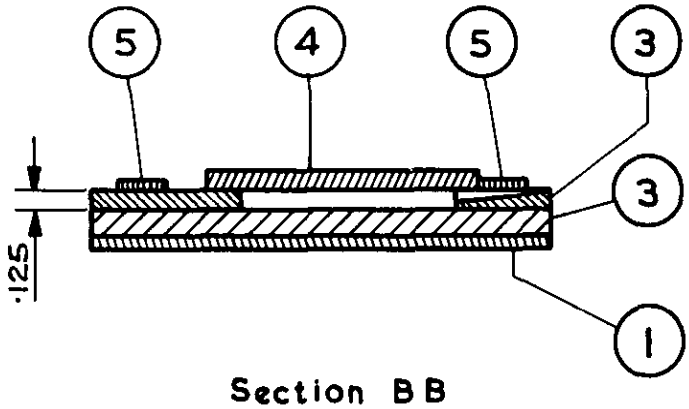

Section B B

Fig. 19 Encapsulation mould

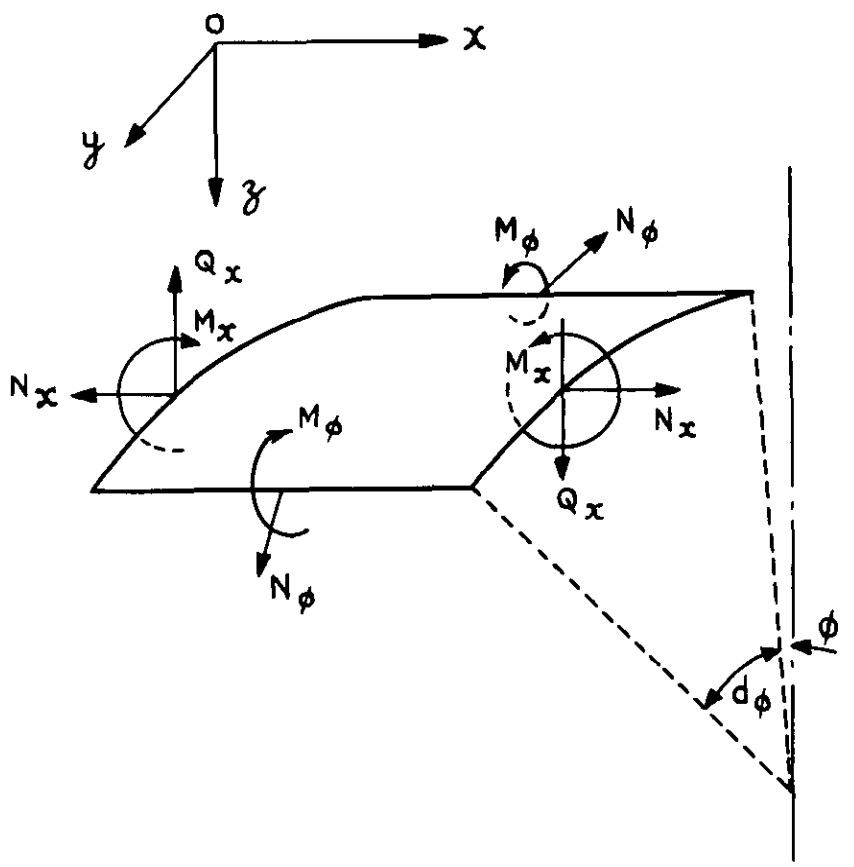

Fig. 20 Stress resultants on the cylindrical shell

Printed in England for Her Majesty's Stationery Office by the Royal Aircraft Establishment, Farnborough Dd 501371 K 4

DETACHABLE ABSTRACT CARD

A.R.C. C.P.1117
February 1969

Stone, D. E. W.
Baxter, P. S. A.

533.6.071.1 :
533.6.048.6 :
531.218 :
531.259.223 :
539.319

AN INVESTIGATION OF THE STRESSES IN A WIND TUNNEL CORNER SECTION

This Report describes how the stresses in a wind tunnel corner section were investigated by means of a 1/6 scale model. Both the brittle coating technique and elevated temperature strain gauges were employed. Two separate tests were performed in which it was attempted to simulate the thermal stresses and the pressure stresses respectively. Methods of overcoming some interesting experimental problems are fully reported and the significance of the results obtained is discussed.

A.R.C. C.P.1117
February 1969

Stone, D. E. W.
Baxter, P. S. A.

533.6.071.1 :
533.6.048.6 :
531.218 :
531.259.223 :
539.319

AN INVESTIGATION OF THE STRESSES IN A WIND TUNNEL CORNER SECTION

This Report describes how the stresses in a wind tunnel corner section were investigated by means of a 1/6 scale model. Both the brittle coating technique and elevated temperature strain gauges were employed. Two separate tests were performed in which it was attempted to simulate the thermal stresses and the pressure stresses respectively. Methods of overcoming some interesting experimental problems are fully reported and the significance of the results obtained is discussed.

Published by
HER MAJESTY'S STATIONERY OFFICE

To be purchased from
49 High Holborn, London W.C 1
13a Castle Street, Edinburgh EH2 3AR
109 St. Mary Street, Cardiff CF1 1JW
Brazennose Street, Manchester 2
50 Fairfax Street, Bristol BS1 3DE
258 Broad Street, Birmingham 1
7 Linenhall Street, Belfast BT2 8AY
or through any bookseller

C.P. No. 1117

SBN 11 470305 1